

 Open access • Posted Content • DOI:10.1101/2021.06.17.21258371

ADESSO detects SARS-CoV-2 and its variants: extensive clinical validation of an optimised CRISPR-Cas13-based COVID-19 test — [Source link](#)

[Casati B](#), [Verdi Jp](#), [Hempelmann A](#), [Kittel M](#) ...+10 more authors

Institutions: [Heidelberg University](#), [German Cancer Research Center](#)

Published on: 22 Jun 2021 - [medRxiv](#) (Cold Spring Harbor Laboratory Press)

Topics: [Population](#)

Related papers:

- [Clinical validation of RCSMS: a rapid and sensitive CRISPR-Cas12a test for the molecular detection of SARS-CoV-2 from saliva](#)
- [Rapid detection of SARS-CoV-2 by pulse-controlled amplification \(PCA\).](#)
- [SARS-CoV-2 detection by a clinical diagnostic RT-LAMP assay](#)
- [RT-qPCR assay for detection of British \(B.1.1.7\) and South Africa \(B.1.351\) variants of SARS-CoV-2](#)
- [Equipment-free detection of SARS-CoV-2 and Variants of Concern using Cas13](#)

Share this paper:    

View more about this paper here: <https://typeset.io/papers/adesso-detects-sars-cov-2-and-its-variants-extensive-3au7ilpoux>

1 **TITLE:**

2 ADESSO detects SARS-CoV-2 and its variants: extensive clinical validation of an optimised
3 CRISPR-Cas13-based COVID-19 test

4
5 **AUTHORS**

6
7 Beatrice Casati^{1,2}, J.P. Verdi^{1,3}, A. Hempelmann³, Maximilian Kittel^{4,6}, Andrea Gutierrez
8 Klaebisch^{5,6}, Sybille Welker^{5,6}, Sonal Asthana¹, Pavle Boskovic⁷, Ka Hou Man⁷, Bernhard
9 Radlwimmer⁷, C. Erec Stebbins³, Thomas Miethke^{*,5,6}, F. Nina Papavasiliou^{*,1}, Riccardo
10 Pecori^{*,1}

11
12 * These corresponding authors contributed equally.

13
14 **AFFILIATIONS**

15
16 ¹Division of Immune Diversity, Department of Immunology and Cancer, German Cancer
17 Research Centre (DKFZ), 69120 Heidelberg, Germany.

18 ²Faculty of Biosciences, Heidelberg University, 69120 Heidelberg, Germany.

19 ³Division of Structural Biology of Infection and Immunity, Department of Immunology and
20 Cancer, German Cancer Research Centre (DKFZ), 69120 Heidelberg, Germany.

21 ⁴Institute of Clinical Chemistry, Medical Faculty of Mannheim, University of Heidelberg,
22 Theodor-Kutzer-Ufer 1-3, 68167 Mannheim, Germany

23 ⁵Institute of Medical Microbiology and Hygiene, Medical Faculty of Mannheim, University of
24 Heidelberg, Theodor-Kutzer-Ufer 1-3, 68167 Mannheim, Germany

25 ⁶Mannheim Institute for Innate Immunoscience (MI3), Medical Faculty of Mannheim, University
26 of Heidelberg, Ludolf-Krehl-Str. 13–17, 68167 Mannheim, Germany

27 ⁷Division of Molecular Genetics, German Cancer Research Centre (DKFZ), 69120 Heidelberg,
28 Germany.

29
30 **IMPORTANT NOTE: This protocol should not be used for clinical purposes. Although we**
31 **have validated the protocol on patient samples, this test is not officially authorized. We**
32 **hope this protocol will provide some reference points for researchers interested in**
33 **further advancing Crispr-DX diagnostic platforms. We also welcome researchers to**
34 **contact us for any assistance.**

35
36 **ABSTRACT**

37
38 With the coronavirus disease 19 (COVID-19) pandemic now deep into its second year,
39 widespread testing for the detection of the causative severe acute respiratory syndrome
40 coronavirus 2 (SARS-CoV-2) is fundamental. The gold standard reverse transcription
41 quantitative PCR (RT-qPCR) cannot keep up with the high demand alone, therefore alternative
42 diagnostic tests are needed. Here we present ADESSO (Accurate Detection of Evolving SARS-
43 CoV-2 through SHERLOCK Optimisation), an optimised version of the CRISPR-based
44 SHERLOCK (Specific High-sensitivity Enzymatic Reporter unLOCKing) assay. After an

45 extensive validation on 983 clinical samples, we demonstrated that ADESSO has a sensitivity of
46 96% and a specificity of 100% on extracted RNA, comparable to RT-qPCR. Its performance on
47 unextracted samples still allows the detection of the more infectious 75% of the COVID-19
48 positive population, making it suitable for point-of-care (POC) testing. Interestingly, our in
49 parallel comparison of 390 matching swab and gargle samples showed consistently lower viral
50 loads in gargle specimens. We also validated ADESSO for the detection of the B.1.1.7 variant
51 and demonstrated that ADESSO is adaptable to any variant of concern in less than one week, a
52 critical feature now that worrisome SARS-CoV-2 variants are spreading all around the world.

53

54 INTRODUCTION

55

56 Since the beginning of the global pandemic of coronavirus disease 2019 (COVID-19),
57 170 million confirmed cases, including 3.5 million deaths, have been reported¹. COVID-19 is a
58 severe respiratory disease caused by severe acute respiratory syndrome coronavirus 2 (SARS-
59 CoV-2)^{2,3,4}. The quick diffusion of SARS-CoV-2 is primarily attributed to the relatively long
60 duration of viral shedding by infected individuals, the viral load dynamics and the lengthy
61 incubation period⁵. Indeed, the incubation period of SARS-CoV-2 is estimated to be 5-6 days^{6,7}
62 with a high viral load upon the onset of symptoms⁸⁻¹⁰, suggesting that individuals with COVID-
63 19 begin viral shedding a few days before symptoms appear¹¹. Further, a significant proportion
64 of infected individuals either remain entirely asymptomatic or only manifest mild symptoms¹²⁻¹⁴.
65 Since these carriers are still able to transmit the virus, case identification and contact tracing
66 protocols alone remain inefficient^{11,13,15-18}, thus facilitating uncontrolled spread of the virus and
67 leading to the current pandemic situation.

68 The urgent need for a vaccine has accelerated the development of multiple effective
69 vaccines and more than 1.5 billion doses have already been administered^{1,19-22}. However, even
70 in the most optimistic scenario, it will take some time before we will be able to reap the benefit of
71 a global vaccination campaign^{23,24}. Therefore, complementary efforts to limit the spread of the
72 virus are still essential.

73 To mitigate viral spreading, many countries adopted extreme social distancing
74 measures, including strict lockdowns²⁵. However, the socio-economic costs for such measures
75 are enormous and the consequences will be long lasting²⁶⁻²⁸. Therefore, the highest priority has
76 to be given to the development of strategies aimed at ensuring long-term safety through
77 containment and isolation of SARS-CoV-2 positive individuals and, at the same time, allowing a
78 safe restart of businesses and social life²⁹. A recent model of viral dynamics suggests that
79 frequent testing for the identification of viral infections and the isolation of carriers is essential³⁰.
80 Notably, the model indicates that effective screening depends mainly on the frequency of testing
81 and speed of reporting, while only to some extent on test sensitivity³⁰.

82 The worldwide gold standard diagnostic test for SARS-CoV-2 infection is the reverse
83 transcription quantitative polymerase chain reaction (RT-qPCR). Viral RNA is isolated from
84 nasal swabs, throat swabs or saliva, retro-transcribed into cDNA and specific regions of the viral
85 genome are amplified via quantitative PCR. Multiple primer sets are utilised, allowing for the
86 amplification of different targets with a LoD of 10³ viral RNA cp/ml³¹.

87 An important limitation of RT-qPCR is the requirement for specific equipment, laboratory
88 infrastructures and qualified personnel. Inadequate access to such resources significantly

89 reduces the frequency of testing. Additionally, PCR testing facilities often require days' worth of
90 time to report the test outcome, resulting in a long sample-to-result turnaround time. To face
91 these challenges, different rapid tests have been implemented, such as rapid PCR and antigen-
92 based tests. However, since rapid PCR tests still require specific equipment and antigen-based
93 tests have lower sensitivity and specificity³², there is a need for an alternative test that is
94 comparable to RT-qPCR in terms of sensitivity and specificity, but faster and independent of
95 complex instruments.

96 All these requirements are met by the so-called CRISPR diagnostic (CRISPR Dx)
97 technologies, which comprise multiple tools for rapid, economical, sensitive and specific nucleic
98 acid detection³³. The CRISPR system is a bacterial machinery able to recognise and cleave
99 foreign genetic material. Among the CRISPR associated (Cas) proteins, Cas13 and Cas12 are
100 able to specifically bind RNA and DNA molecules, respectively, complementary to the target-
101 binding CRISPR RNA (crRNA). Upon target recognition, the Cas proteins cleave a reporter in
102 *trans*, which can then be detected via different readouts³⁴⁻³⁶. These readouts are limited by the
103 amount of detectable target material in the sample of interest. To circumvent this limitation,
104 isothermal amplification methods that do not rely on sophisticated equipment, such as loop-
105 mediated isothermal amplification (LAMP)³⁷ or recombinase polymerase amplification (RPA)³⁸
106 have been combined with Cas-mediated nucleic acid detection^{35,39,40}. CRISPR Dx technologies
107 were quickly adapted to offer point-of-care (POC) diagnostic tests for the detection of SARS-
108 CoV-2. In about an hour, test results can be read on paper-based lateral flow sticks or by
109 fluorescence detection with portable devices⁴¹⁻⁴⁸. Despite the high potential of CRISPR Dx
110 technologies, only two of them have received emergency use authorisation from the Food and
111 Drug Administration (FDA), with use restricted to the authorised laboratories^{49,50}. The analysis of
112 their performance on clinical samples is still not adequate enough to grant them approval for
113 use in routine diagnostics, therefore a more extensive study in comparison with RT-qPCR is
114 necessary.

115 Here we have optimised the Cas13a-based detection platform named "SHERLOCK"^{39,40}
116 and developed ADESSO (Accurate Detection of Evolving SARS-CoV-2 through SHERLOCK
117 Optimisation) for highly sensitive detection of SARS-CoV-2 directly from patient-derived
118 material. The entire protocol takes one hour, does not require RNA extraction or any specific
119 equipment, is able to detect down to 2.5 cp/μl of SARS-CoV-2 synthetic genome and is low-cost
120 (less than 5€ per test). Throughout our work we extensively evaluated the real diagnostic
121 potential of ADESSO in direct comparison to RT-qPCR and with two different sample collection
122 methods (nasopharyngeal swab (NP) vs gargle of saline). Importantly, all the samples were
123 collected from ambulatory patients presenting minimal or mild symptoms or from people
124 identified as contacts of SARS-CoV-2 infected individuals, representing a part of the population
125 that can potentially remain undetected. Our study showed that ADESSO has a sensitivity
126 comparable to RT-qPCR when applied to purified RNA, while it resulted in a lower sensitivity
127 when performed directly on unextracted samples, yet still being more sensitive than rapid
128 antigen tests³². However, considering that the Ct values across our cohort follow a normal
129 distribution, we can fairly estimate that ~75% of the entire infected population would be
130 successfully detected by ADESSO on unextracted swabs. Importantly, the 25% portion of
131 infected individuals that ADESSO would miss corresponds to high RT-qPCR Ct values,
132 coinciding with low viral titers and minimal infectiousness^{11,51}. Additionally, we also observed a

133 drop in sensitivity when gargling was used as sampling method for both ADESSO and RT-
134 qPCR. Finally, in less than one week we adapted ADESSO to specifically identify SARS-CoV-2
135 variants in clinical samples by modifying the primers and crRNAs used for amplification and
136 detection. The adapted ADESSO can identify the presence of a variant within one hour of
137 sample submission, thus eliminating the need for sequencing, while RT-qPCR tests would
138 require an additional day or two on top of the already slower turnaround. Considering the risk
139 posed by the spread of the new SARS-CoV-2 variants, this feature is highly relevant in the
140 current phase of the COVID-19 pandemic and in the near future⁵².

141

142

143 RESULTS

144

145 A SHERLOCK-based assay for SARS-CoV-2 detection in clinical samples

146 The need for a rapid and sensitive COVID-19 POC test has been and will remain a significant
147 factor to contain the spread of SARS-CoV-2. CRISPR Dx technologies represent a viable option
148 for the development of such a test³³. For this reason, we first aimed to reproduce and adapt a
149 Cas13-based molecular detection platform called SHERLOCK (Specific High Sensitivity
150 Enzymatic Reporter UnLOCKing)³⁹ for the detection of SARS-CoV-2 in clinical samples.
151 SHERLOCK is based on two main steps: (a) isothermal amplification of viral RNA via RT-RPA
152 and (b) detection of a specific RNA sequence by Cas13 protein followed by *trans*-cleavage of a
153 labeled reporter, which can be detected via a lateral flow-based visual readout³⁹ (**Figure 1A**).
154 During the RT-RPA, RNA is retro-transcribed and amplified to dsDNA using specific primers³⁸
155 and a T7 promoter is added to the amplicon by including its sequence in the forward primer.
156 This feature is necessary for the Cas13 detection step, where a T7 RNA polymerase transcribes
157 the amplified dsDNA back into RNA, which can be specifically recognised by Cas13 protein in
158 complex with a crRNA complementary to the target. The specific binding between the Cas13-
159 crRNA complex and its target RNA activates Cas13 collateral activity, leading to cleavage of an
160 RNA reporter and generation of a detectable signal. Finally, the resulting signal can be read on
161 a lateral flow-based visual readout. For this readout an RNA reporter flanked by biotin and
162 fluorescein (FAM) is used in combination with anti-FAM antibodies labelled gold nanoparticles
163 used to visualise the reporter. In a negative sample, the reporter is intact and is captured by a
164 line of streptavidin resulting in a first band called “control band”. In a positive sample, the
165 reporter is cut, therefore the first half of the reporter containing biotin is captured by streptavidin,
166 while the other half containing FAM is captured by a second line of antibodies resulting in the
167 appearance of the so-called “test band”. The band intensity ratio between the test band and the
168 control band indicates the portion of reporter that has been cut, which reflects the level of Cas13
169 activation and thus the amount of target RNA that was detected in the sample (**Figure 1A**).

170 We first generated SARS-CoV-2-specific guide sequences, purified LwaCas13a protein⁵³
171 (**Figure S1A,B**) and tested the system’s detection sensitivity in the absence of a pre-
172 amplification step using serial dilutions of an *in-vitro*-transcribed (IVT) fragment of the SARS-
173 CoV-2 S gene. As previously published, a sensitivity of 10⁸ aM was observed³⁹ (**Figure S1C**).
174 We then assessed the sensitivity of our test when combining the Cas13 detection with an RT-
175 RPA pre-amplification step on SARS-CoV-2 genes S and Orf1a, as formerly described⁵⁴. A 2-
176 fold improvement of the previously published sensitivity was obtained⁵⁴. Indeed, we detected

177 SARS-CoV-2 gene S at a concentration of 10aM (5 cp/μl) and gene Orf1a at a concentration of
178 100aM (50 cp/μl) (**Figure 1B**). This improvement is most likely due to the replacement of
179 ProtoScript II Reverse Transcriptase (RT) with M-MuLV RT, which retains a functional RNase H
180 domain that degrades DNA:RNA hybrid intermediates and thereby improves the efficiency of
181 RT⁵⁵ (**Figure S1D**). We then used the set of primers and crRNA for S to conduct a blind test on
182 30 clinical samples. These samples were NP swabs collected in saline (0.9% NaCl) and they
183 were previously tested for SARS-CoV-2 via RT-qPCR (Roche Cobas System) at the Medical
184 University Hospital Mannheim. The specimens were frozen and transported to our laboratory,
185 where we extracted RNA and performed SHERLOCK in duplicates. Additionally, the CDC 2019-
186 nCoV Real-Time RT-PCR Diagnostic Panel⁵⁶ was also performed as a control. Using
187 SHERLOCK, we were able to identify all 10 positive samples (**Figure 1C, Table S1**). Notably,
188 we detected sample 28, which had a very low viral titer (corresponding to a high Ct value).
189 These results demonstrate that SHERLOCK can be used as an alternative method to detect
190 SARS-CoV-2 in RNA extracted from clinical samples.

191

192

193 **SARS-CoV-2 direct detection from clinical samples**

194 RNA extraction is a time-consuming, labor-intensive and costly step for COVID-19 diagnosis
195 (**Figure 1A**) and shortage of RNA extraction kits has been a global issue throughout the
196 pandemic^{57,58}. Different studies have already demonstrated that it is possible to omit it^{41,43,59,60}.
197 Therefore, after demonstrating the high potential of SHERLOCK as a diagnostic test for COVID-
198 19, we attempted to improve our protocol in order to avoid the RNA extraction step, thus making
199 the test faster and cheaper (**Figure 2A**). First, we compared different lysis methods by treating
200 one known positive sample (sample #30 in **Figure 1C** and **Supplementary File 1**) with either
201 QuickExtract DNA Extraction solution (Lucigen, #QE09050), Luna Cell Ready Lysis Buffer
202 (NEB, #E3032) or 5% Triton X 100 (Carl Roth, #3051.3) and incubating it for 5 min at 95°C. We
203 performed the experiment in triplicates for each lysis method and we were able to successfully
204 detect SARS-CoV-2 directly after lysing the sample with QuickExtract DNA Extraction solution
205 and Luna Cell Ready Lysis Buffer (**Figure 2B**). Lysis with 5% Triton X 100 did not allow SARS-
206 CoV-2 detection, although it was successfully performed in another study⁵⁹. To improve the
207 sensitivity of our test, we first optimised the amount of RT units and sample input in the RT-RPA
208 step using dilutions of synthetic SARS-CoV-2 genome. We observed the best results with 6 U/μl
209 of RT and 2.5 μl of sample input per reaction (**Figure S2A**). Additionally, we compared our
210 standard set of RPA primers and Cas13 crRNA for S with other sets designed to target different
211 genes of SARS-CoV-2, namely N and Orf1a. First, we assessed their performance on serial
212 dilutions of a positive sample (sample #6 in **Figure 1C** and **Supplementary File 1**) (**Figure**
213 **S2B**). Then, we compared the sensitivity of the best two candidates, S and Orf1a, on dilutions of
214 synthetic SARS-CoV-2 genome⁶¹. The set of RPA primers and Cas13 crRNA for S remained the
215 most sensitive one (**Figure S2C**). We therefore selected it for all the following experiments. In
216 order to assess the sensitivity of our test on unextracted samples, we spiked in serial dilutions of
217 SARS-CoV-2 synthetic genome in a negative sample lysed with QuickExtract solution and we
218 performed SHERLOCK on the S gene. We were able to consistently detect 10 cp/μl (**Figure**
219 **2C**). We then proceeded with the evaluation of the diagnostic potential of SHERLOCK on
220 unextracted samples (so-called direct SHERLOCK) by performing a second blind test on 160

221 clinical samples. Positive samples were considered those which resulted in a band intensity
222 ratio (test band/control band) higher than 0.2. This threshold was defined based on the band
223 intensity ratio obtained in all the negative controls used in this study and the negative samples
224 analysed in Figures 2 and 4 (n = 282 + 467; **Figure S3A**). Direct SHERLOCK was able to
225 identify 73 out of 93 positive samples resulting in a sensitivity of 78% (**Figure 2D,E** and **Table**
226 **S1**). Importantly, despite an apparent LoD equivalent to Ct 27, samples with lower Ct values
227 and high viral loads resulted in a highly variable band intensity ratio with some being very close
228 to the 0.2 threshold (**Figure 2D**). For this reason, we decided to proceed with a step-by-step
229 optimisation of the direct SHERLOCK protocol.

230

231

232 **ADESSO: an optimised and highly sensitive SHERLOCK assay**

233 Considering the results of the detection of SARS-CoV-2 directly from clinical samples (**Figure**
234 **2**), we aimed at optimising the SHERLOCK protocol to develop a direct SARS-CoV-2 diagnostic
235 test that is as sensitive as possible. Therefore, we evaluated alternative reagents and different
236 reaction conditions for each one of the three main steps in SHERLOCK, namely, 1) sample
237 lysis, 2) RT-RPA and 3) Cas13 detection (**Figure S4A**), to increase both sensitivity and speed
238 of the test. At this stage, we assessed Cas13 activation also via a fluorometer to monitor the
239 speed of the reaction in real time. The fluorescence readout is based on the use of an RNA
240 reporter flanked by a fluorophore and a quencher. Upon Cas13-mediated cleavage of the
241 reporter, the fluorophore is cut from the quencher and its fluorescent signal can be detected by
242 a fluorometer (**Figure S4A**). First, we measured the RNase activity in a swab sample collected
243 in saline and lysed with the method selected in Figure 2 (QuickExtract DNA Extraction solution
244 and incubation at 95°C for 5 min). To evaluate RNase activity, RNaseAlert was added to the
245 sample following lysis and fluorescence was measured to evaluate the corresponding nuclease
246 activity. Notably, addition of RNase inhibitors in the lysis buffer prior to heating was sufficient to
247 inhibit RNase activity almost completely (**Figure 3A**). Next, we optimised the RT-RPA step by
248 first comparing different RT enzymes in the presence or absence of RNase H. Once again, M-
249 MuLV shows the best sensitivity (5-2.5 cp/μl) in comparison to ProtoScript II or SuperScript III,
250 while the addition of RNase H leads to an improvement for SuperScript III only (**Figure 3B**).
251 Secondly, we used different final concentrations of RPA, where 1xRPA corresponds to the
252 standard amount of RPA described in the original SHERLOCK protocol^{39,53,54} and 5xRPA
253 corresponds to the optimal amount according to the manufacturer's instructions. To test this, we
254 selected one false negative sample from our previous blind test on unextracted samples
255 (sample #L151, **Supplementary File 1**) and a true negative sample as negative control (sample
256 #L126, **Supplementary File 1**) and we repeated our assay with different concentrations of RPA.
257 Remarkably, while the false negative sample is still negative with 1xRPA, it results positive for
258 final concentrations of RPA from 2x to 5x, with a decrease in band intensity ratio when using the
259 4xRPA and 5xRPA concentrations (**Figure 3C, S4B**). Considering this and bearing in mind the
260 cost per single test, we decided to proceed using a 2xRPA concentration. To further confirm this
261 improvement, we compared 1xRPA and 2xRPA on 5 samples with Ct values close to the LoD
262 determined in Figure 2 (samples #L95, L96, L111, L122 and L123, **Supplementary File 1**). We
263 observed an improvement in the 2xRPA reactions with these samples as well (**Figure 3D, S4C**).
264 Furthermore, in order to optimise the Cas13 detection step we made a ten-fold dilution of a

265 positive RT-RPA reaction (50 cp/μl) and we performed Cas13 detection using the original
266 concentration of Cas13/crRNA (45/22.5 nM)^{39,53,54}, in comparison to higher amounts (**Figure**
267 **S4D**, upper panel). A concentration of Cas13/crRNA of 90 nM each leads to an improved
268 reaction, reaching the plateau after 15 min only, compared to 30 min for the other two
269 concentrations (**Figure 3E, S4D**, lower panel). We also confirmed that a 10-min incubation for
270 Cas13 detection performed in half the volume is sufficient to yield a clearly positive outcome in
271 the lateral flow detection assay (**Figure 3F, S4E**), which is an essential aspect for a POC test.
272 Moreover, a shorter Cas13 reaction allows us to extend the incubation time of the RT-RPA step
273 for highly sensitive reactions⁵³ without affecting the total time of the assay. Finally, we assessed
274 the sensitivity of this optimised protocol on serial dilutions of SARS-CoV-2 synthetic genome
275 and we observed a robustly reproducible sensitivity of 2.5 cp/μl (**Figure 3G**). We named this
276 new optimised diagnostic assay ADESSO (Accurate Detection of Evolving SARS-CoV-2
277 through SHERLOCK Optimisation) (**Figure 3H**).

278
279

280 **Evaluation of ADESSO performance on clinical samples in direct comparison to RT-** 281 **qPCR.**

282 We used ADESSO to test a total of 195 clinical samples in direct comparison to the RT-qPCR
283 protocol routinely used in the clinics. To allow a fair comparison between the methods, we first
284 selected 95 positive and 100 negative individuals (via COBAS RT-qPCR on NP swab). For each
285 of these specimens, RNA was re-extracted and analysed by RT-qPCR (Tib Molbiol) and
286 ADESSO. Additionally, ADESSO was also performed directly on unextracted samples. Finally,
287 we also obtained gargled saline from the same individuals as an alternative sampling method,
288 which would be ideal for POC testing. Those samples were treated exactly as the NP swabs
289 (**Figure 4A**). Importantly, the ADESSO results were analysed without knowing the outcome of
290 the COBAS RT-qPCR used as the reference.

291 The results of this experiment are summarised in **Table 1**. ADESSO on RNA extracted from
292 swabs was able to correctly identify most positive samples (91 out of 95), resulting in a
293 sensitivity of 96% (**Figure 4B**). Interestingly, all the false negative samples have Ct values
294 higher than 31, corresponding to lower viral loads (<100cp/μl) and therefore a lower probability
295 of spreading the virus^{11,51}. RT-qPCR (Tib Molbiol) performed on the same samples was largely
296 in agreement with the COBAS RT-qPCR, with highly correlated Ct values (**Figure 4F**).
297 However, using this method we were able to identify 89 out of 95 positive samples resulting in a
298 sensitivity of 94% (**Table 1** and **Figure 4F**). As expected, ADESSO on unextracted samples
299 resulted in a lower sensitivity (77%), with all false negative samples having Ct values higher
300 than 29 (~100cp/μl) (**Table 1** and **Figure 4C**). The same analysis was performed on gargle
301 saline samples. In this case, ADESSO on extracted RNA correctly identified 74 out of 95
302 positive samples resulting in a sensitivity of 78%, with most false negative samples having Ct
303 values higher than 30 and few with Ct values between 28 and 29 (**Figure 4D**). Interestingly, this
304 drop in sensitivity does not seem to be related to the detection method but rather to the
305 sampling method. Indeed, the same decrease in sensitivity (to 79%) was observed also for RT-
306 qPCR (TibMolBio), with true positive samples resulting in higher Ct values (**Table 1** and **Figure**
307 **4G**). Finally, as observed for swabs, ADESSO on unextracted gargle saline samples resulted in
308 a lower sensitivity (65%) (**Figure 4E** and **Table 1**). In this latter case, false negative samples

309 have different Ct values, with some corresponding to high viral loads in swabs (analysed by
310 COBAS RT-qPCR) (dark red dots in **Figure 4E** and **4H**). The overall decrease in sensitivity is in
311 agreement with the consistently higher Ct values observed in gargle specimens compared to
312 their matched swab samples analysed via Tib Molbiol RT-qPCR (**Figure 4H**).

313 Altogether, these results validate the high potential of ADESSO as a POC test for the detection
314 of SARS-CoV-2 infected individuals. Notably, ADESSO on extracted RNA, either from swab or
315 gargle samples, performed as well as RT-qPCR (Tib Molbiol) in terms of sensitivity and
316 specificity. Additionally, our data also shows an important difference in the detection of SARS-
317 CoV-2 when gargling with saline was used as a sampling method. Even though this approach
318 would be better suited to a POC test, we observed a clear reduction in sensitivity, independently
319 of the detection method used.

320 321 **Adaptation of ADESSO for detection of SARS-CoV-2 variants: a flexible and powerful** 322 **assay to rapidly identify specific variants or mutations.**

323 Since the beginning of the pandemic, SARS-CoV-2 has evolved considerably. The first variants
324 to appear carried a D614G mutation in the spike protein⁶², which is now dominant and shared
325 between all the existing variants. While several variants exist, here we focus our attention on
326 two variants of concern: SARS-CoV-2 B.1.1.7 (UK variant) and SARS-CoV-2 B.1.351 (South
327 Africa (SA) variant). SARS-CoV-2 B.1.1.7, also known as 501Y.V1, seems to have an enhanced
328 transmissibility⁶³ and might be more virulent⁶⁴. It was first detected in England in late 2020 and,
329 after becoming the dominant variant in the UK, it has spread quickly all over Europe and
330 worldwide. B.1.1.7 contains eight mutations in the spike gene in addition to the mutation causing
331 the D614G substitution, including deletions (e.g., Δ HV69-70) (**Figure 5A**). SARS-CoV-2
332 B.1.351, also known as 501Y.V2, was first detected in late 2020 in Eastern Cape, South
333 Africa⁶⁵. This variant quickly became dominant locally and displaced other viral lineages in
334 several regions, possibly as a result of increased transmissibility or immune escape^{65,66}. B.1.351
335 contains nine mutations in the spike gene in addition to the mutation causing the D614G
336 substitution, including clusters of mutations (e.g., mutations leading to Δ 242-244 and R246I)
337 (**Figure 5A**). Finally, there is growing evidence that these new variants could impair the efficacy
338 of current monoclonal antibody therapies and vaccines because of the several mutations
339 located in the spike gene⁶⁷⁻⁶⁹. For this reason, it is now essential to quickly identify individuals
340 infected by SARS-CoV-2 variants. The UK variant is the major concern in Europe and Germany,
341 therefore we adapted our test to detect the deletion (Δ HV69-70) specific to this strain. We called
342 this adapted test ADESSO-UK (**Figure 5A,B**). First, we designed two different crRNAs able to
343 recognise either the original Wuhan strain or the UK variant, called respectively crRNA HV69-70
344 and crRNA Δ HV69-70 (**Figure 5B**). Then we optimised RT-RPA primers to amplify the region of
345 SARS-CoV-2 genome containing HV69-70 and we selected the more sensitive set 1 for further
346 analysis (**Figure S5A**). Finally, we performed a blind test on positive clinical samples carrying
347 either UK or SA variants. We first applied ADESSO for the detection of SARS-CoV-2 and we
348 were able to detect all positive samples but one (sample #11, **Figure 5C**). Then, using
349 ADESSO-UK (crRNA Δ HV69-70 or HV69-70) we were able to correctly identify all the samples
350 carrying the UK variant and we could distinguish the ones bearing the SA strain (samples #1-13,
351 **Figure 5D,E** and **S5B**). Interestingly, among the three samples carrying the SA variant, only
352 sample #11 was not detected via ADESSO. Sequencing analysis of the viral genome in these

353 three samples showed that they all shared the deletion $\Delta 242-244$, but only sample #11 carried
354 the R246I mutation (**Figure S5C**). This mutation falls exactly within the bases recognised by the
355 3' end of the forward primer used in the RT-RPA step of ADESSO, thus disrupting its function
356 (**Figure 5F**). Notably, the assay seems to be resistant to deletions of several nucleotides
357 occurring in sequences that are complementary to the central region of the primer (**Figure 5F**).
358 Altogether, these results show how ADESSO can be readily adapted for the detection of SARS-
359 CoV-2 variants of concern and even specific mutations. The entire adaptation of the test took
360 less than one week, from the selection of a unique mutation for the UK variant to the validation
361 of the adapted protocol, including designing and production of the specific reagents. This
362 feature of our assay is a crucial aspect in the current phase of the COVID-19 pandemic, where
363 quick and sequencing-independent detection of variants is essential to contain their spread⁵².

364

365

366 **DISCUSSION**

367

368 The COVID-19 pandemic has been afflicting the world for more than a year now and the
369 number of new weekly global cases is still hitting its highest levels, despite multiple effective
370 vaccines being distributed¹. Therefore, promptly tracking infected individuals to isolate them and
371 prevent further spread of the virus is fundamental. The gold-standard RT-qPCR-based COVID-
372 19 diagnostic test alone cannot keep up with the high demand for testing and the long
373 turnaround time is an issue when a fast response is essential. Rapid PCR and antigen-based
374 tests are also available, but there are some limitations for their widespread use, such as the
375 requirement for sophisticated PCR equipment and the standard practice of confirming positive
376 antigen-based test results by RT-qPCR. Therefore, an alternative test that overcomes these
377 limitations is still needed. Here, we have optimised the Cas13a-based diagnostic platform called
378 SHERLOCK³⁹ and developed the improved protocol ADESSO for highly sensitive COVID-19
379 testing. Overall, we tested 983 samples (496 positive and 487 negative, **Supplementary File**
380 **1**), in parallel comparison with RT-qPCR. To our knowledge, it is the first time that such an
381 extensive study on clinical samples has been reported for CRISPR Dx technologies. ADESSO
382 has a sensitivity of 96% on RNA extracted from swabs and a sensitivity of 77% when performed
383 directly on unextracted swab samples. This drop in sensitivity is due to a decreased LoD at Ct
384 29, corresponding to low viral titers and minimal infectiousness^{11,51}. However, skipping the RNA
385 extraction step considerably reduces the sample-to-result turnaround time and allows more
386 frequent testing, which is suggested to be essential for efficient identification of viral infections
387 and isolation of carriers to contain the pandemic³⁰. Other advantages are the lower need for
388 RNA extraction kits, whose shortage has been a global issue throughout the pandemic^{57,58}, and
389 the higher test portability, which makes ADESSO appropriate for POC testing. To further
390 increase the POC suitability of ADESSO, we assessed its performance in comparison with RT-
391 qPCR on gargle samples obtained from the same individuals from whom swabs were collected.
392 Interestingly, we observed a loss in sensitivity independently of the diagnostic test. On RNA
393 extracted from gargle samples, ADESSO showed a sensitivity of 78%, comparable with a 79%
394 sensitivity of the RT-qPCR. In line with what we observed for swab samples, the sensitivity of
395 ADESSO decreased to 65% when performed directly on unextracted gargle samples (**Table 1**).
396 This overall loss of sensitivity can be attributed to the sampling method, which leads to a

397 general increase in Ct values in gargle samples compared to swabs collected from the same
398 individuals at the same time (**Figure 4H**). To our knowledge, this is the first study that compares
399 two different sampling methods in parallel on such a big cohort of patients (n = 195 swabs + 195
400 gargle samples), thus highlighting a consistent difference in detected viral titers depending on
401 the sampling method used. Despite the fact that multiple studies have shown that high SARS-
402 CoV-2 titers can be detected in saliva^{70,71}, our results show that using gargle samples instead of
403 NP swabs, even if more suitable for POC testing, leads to higher rates of false negative
404 samples, independently of the sensitivity of the downstream diagnostic test. Therefore,
405 alternative methods should be considered and evaluated in comparison to gargling and NP
406 swabbing, for example self-collection of nasal swabs, whose feasibility and reliability are already
407 being investigated⁷².

408 Importantly, the cohort of positive individuals analysed in our study was selected randomly and
409 displays a normal distribution of Ct values, covering the full range of viral titers between Ct 17
410 and Ct 38 (**Figure S6A,B**). This aspect is fundamental for two reasons: first, since the samples
411 analysed in this study were collected from ambulatory patients presenting minimal or mild
412 symptoms or from people identified as contacts of SARS-CoV-2 infected individuals, it highlights
413 the fact that these individuals can manifest high viral loads and therefore be infectious;
414 moreover, it allows the inference of the test performance from the experimental cohort to the
415 entire SARS-CoV-2 infected population. In this way, we could confidently estimate what portion
416 of the population our test would detect. Mathematical models show that successful identification
417 and isolation of 50% of infected individuals (and tracing of their contacts) is already sufficient to
418 flatten the infection curve⁷³. Our test exceeds this fraction in all conditions (**Table 1**), strongly
419 suggesting that immediate and widespread application of ADESSO would be of great help to
420 contain the pandemic. In particular, by applying ADESSO on swab samples without RNA
421 extraction, an estimated ~75% of the infected population would be successfully detected, while
422 ~25% of the infected individuals could be missed (**Figure 4** and **S6A**). Importantly, this 25%
423 portion corresponds to individuals with Ct values higher than 29, associated with low viral titers
424 and minimum infectiousness^{11,51}. Finally, our results show a disagreement between LoD on
425 serial dilutions of synthetic viral genome and LoD in clinical samples. Despite the “synthetic”
426 LoD of 2.5 cp/μl (~Ct 35; **Figure 3**), the real clinical sensitivity of ADESSO corresponds to Ct
427 29-31 (**Figure 4**) and the same is true for other studies although it has never been
428 explicated^{43,46}. This aspect highlights that an extensive validation on real clinical samples
429 covering the full range of viral titers and following a normal distribution, as the one presented
430 here, is necessary to determine the real LoD of a diagnostic test. This is crucial to allow a fair
431 comparison between sensitivities resulting from independent studies, which can be greatly
432 influenced by the choice of the tested population.

433 The importance of testing is further highlighted by the recent emergence of SARS-CoV-2
434 variants, which poses a new threat for humanity, as India's recent tragic crisis has shown^{52,74}.
435 This is of utmost criticality because mutations in the viral genome might impair both molecular
436 and antigen-based tests, thus leading to false negative results. In these situations, being able to
437 promptly adapt a test is fundamental and ADESSO offers such an advantage. Here, in less than
438 a week we adapted the test for the detection of the B.1.1.7 variant. Based on the publicly
439 available SARS-CoV-2 sequences (<https://www.gisaid.org>), ADESSO can be adapted to any

440 variant of concern, thus providing an all-in-one SARS-CoV-2 detection and variant identification
 441 tool without need for sequencing.

442 Finally, we calculated a cost per reaction of 2.64€ and 4.82€ for fluorometric and lateral-flow
 443 detection, respectively (**Supplementary File 2**), which would be even lower at a production
 444 scale. Considering the cost range for a single RT-qPCR reaction⁷⁵, three to eight tests could be
 445 performed with ADESSO for the same price. Moreover, the cost of a thermal cycler needed to
 446 perform RT-qPCR would also be eliminated. Lastly, the use of ADESSO for the detection of
 447 variants would even cut the cost of sequencing. Altogether, ADESSO is cheaper than any RT-
 448 qPCR-based COVID-19 diagnostic test and offers a more accessible option for widespread and
 449 more frequent testing.

450 With the COVID-19 pandemic now deep into its second year, it has become clear that time
 451 plays a critical role in the management of such an emergency. In order to control it, rapid
 452 detection of new infections, quick tracing of contacts, fast vaccine distribution and prompt
 453 reaction to emerging new variants are key-factors. Slowly but undeniably, the race against
 454 SARS-CoV-2 has turned from a sprint into a marathon. If we want to keep up, we need to take
 455 action faster than the virus evolves. The time is now for ADESSO to join the race.

456
 457

Sampling method	Sample	Test	Test result	number			number/total number (percentage)			
				Positive samples (N=95)	Negative samples (N=100)	Total samples (N=195)	Positive predictive value	Negative predictive value	Sensitivity	Specificity
SWAB	RNA	Tib Molbiol RT-qPCR	Positive	89	0	89	89/89 (100%)		89/95 (94%)	
			Negative	6	100	106		100/106 (94%)		100/100 (100%)
		ADESSO	Positive	91	0	91	91/91 (100%)		91/95 (96%)	
			Negative	4	100	104		100/104 (96%)		100/100 (100%)
	Unextracted sample	ADESSO	Positive	73	0	73	73/73 (100%)		73/95 (77%)	
			Negative	22	100	122		100/122 (82%)		100/100 (100%)
GARGLE SAMPLE	RNA	Tib Molbiol RT-qPCR	Positive	75	0	75	75/75 (100%)		75/95 (79%)	
			Negative	20	100	120		100/120 (83%)		100/100 (100%)
		ADESSO	Positive	74	0	74	74/74 (100%)		74/95 (78%)	
			Negative	21	100	121		100/121 (83%)		100/100 (100%)
	Unextracted sample	ADESSO	Positive	62	0	62	62/62 (100%)		62/95 (65%)	
			Negative	33	100	133		100/133 (75%)		100/100 (100%)

458
 459 **Table 1:** Positive and negative predictive values, sensitivity and specificity of ADESSO on swab
 460 and gargle samples with and without RNA extraction.

461

462

463 METHODS

464

465 **Protocols.** The RT-RPA and Cas13 reaction protocols used for each experiment are provided
 466 in **Supplementary File 4** with reference to the corresponding figures. The exact volumes are
 467 given for one single reaction.

468

469 **Reagents and materials.** Detailed information about reagents and material used in this study is
 470 provided in **Supplementary File 3**.

471

472 **Cas13 purification:**

473 Plasmid encoding LwaCas13 (pC013 - Twinstrep-SUMO-huLwCas13a was a gift from Feng
474 Zhang (Addgene plasmid # 90097; <http://n2t.net/addgene:90097>; RRID:Addgene_90097)³⁹ was
475 transformed into Rosetta cells and purified according to established protocols with substantial
476 modification. Single colonies were inoculated into 25 ml Terrific Broth (TB) (100 µg/ml AMP) and
477 grown to an OD of 0.6 at 37°C degrees while shaking at 150 rpm. The suspension was chilled
478 for 30 min at 4°C and subsequently induced with 0.5 mM IPTG and left shaking for an additional
479 16h at 21°C. Cells were harvested by centrifugation at 5 k rpm for 15 min at 4°C. The pellet was
480 resuspended in 4x (wt/vol) supplemented lysis buffer (12 cOmplete Ultra EDTA-free tablets, 600
481 mg of lysozyme and 6 µl of benzoase to lysis buffer (20 mM Tris pH 8.0, 500 mM NaCl, 1 mM
482 DTT)) and lysed by sonication. Lysate was cleared by centrifugation at 10 k rpm for 1h at 4°C.
483 Supernatant was purified using a 1 ml HIS-Trap column (Cytiva) slurry and affinity
484 chromatography was performed using the ÄKTA pure system with lysis buffer for washing steps
485 and an imidazole gradient for elution. After initial purification, the protein sample was incubated
486 with SUMO protease (ThermoScientific) as per the manufacturer's instructions at 4°C overnight
487 to remove the affinity tags. The sample was then re-applied to a 1 ml HIS-Trap column. Both the
488 SUMO protease (which itself has a 6xHIS tag) and the cleaved affinity tag bind to the resin,
489 while pure Cas13 eluted in the wash step. A final size-exclusion chromatography step was
490 performed using the ÄKTA pure system using 10 mM HEPES pH 7.0, 5 mM MgCl₂, 1 M NaCl
491 and 2 mM DTT as gel filtration buffer on a Superdex 16/600 column.

492

493 **Synthetic SARS-CoV-2 RNA**

494 Fully synthetic SARS-CoV-2 RNA was purchased from Twist Biosciences (MT007544.1 or
495 MN908947.3). In order to test SHERLOCK sensitivity, serial dilutions were prepared in water or
496 in saline, from the initial concentration of 10⁶ cp/µl to 0.01 cp/µl.

497 **Synthetic SARS-CoV-2 S gene and Orf1ab gene RNA fragments**

498 SARS-CoV-2 RNA, a kind gift of Prof. Bartenschlager (DKFZ, Heidelberg), was used for
499 OneStep RT-PCR (Qiagen, #210212) as follows: 11 µl of nuclease-free water, 5 µl of 5x
500 OneStep RT-PCR buffer, 1 µl of dNTP mix (10mM each), 1.5 µl of each primer (forward and
501 reverse, both 10µM) and 1 µl of OneStep RT-PCR Enzyme Mix were added to 4 µl of denatured
502 RNA. The primers used for the amplification of SARS-CoV-2 S gene and Orf1a gene are listed
503 in **Supplementary File 3**. The RT-PCR protocol was run as follows: retrotranscription at 50°C
504 for 30 min, denaturation at 95°C for 15 min, followed by 40 cycles of denaturation at 94°C for 30
505 sec, annealing at 61°C (Orf1a gene) or 62°C (S gene) for 30 sec and elongation at 72°C for 5
506 sec. In the end a final elongation step at 72°C was run for 10 min. PCR clean-up was performed
507 on the RT-PCR products according to the manufacturer's instructions (Macherey-Nagel,
508 #740609.250). The purified DNA was in-vitro-transcribed into RNA with the HiScribe T7 Quick
509 High Yield RNA Synthesis Kit (NEB, #E2050S) following the suggested protocol for short
510 transcripts. The IVT products were then treated with DNase I (HiScribe T7 Quick High Yield
511 RNA Synthesis Kit, NEB, #E2050S) and purified with Monarch RNA Cleanup Kit (NEB,
512 #T2050). The concentration of the purified products was determined by Nanodrop and Qubit. In
513 order to test SHERLOCK sensitivity, serial dilutions were made in water from a concentration of
514 1µM to 1aM.

515 **Human clinical specimen collection**

516 Clinical specimens were collected at the Medical University Mannheim, Germany. NP swabs
517 and gargle samples were collected from ambulatory patients presenting minimal to mild
518 symptoms or sent by the German Health Department after having contact with a SARS-CoV-2
519 positive person. After verbal and visual instruction gargling was performed with 8 ml of sterile
520 0,9% saline (Fa. Fresenius Kabi, Bad Homburg, Germany). Samples were collected in sterile
521 containers without additives and stored at 4°C until testing with PCR within 36 h. NP specimens
522 were collected with flocked swabs (Improswab, Fa. Improve Medical Instruments,
523 Guanzhou/China) and washed out with 2 ml 0,9% saline within 12 h of collection. For sample
524 inclusion in the validation study and side-by-side comparison of ADESSO and RT-qPCR, initial
525 PCR was performed on NP swab samples as part of routine clinical care using the cobas 6800
526 system (Roche, Penzberg, Germany) according to the manufacturer's instructions. Based on
527 the results of the initial PCR, 95 positive and 100 negative samples were selected.

528

529 **RNA extraction**

530 For the first blind test (Figure 1), RNA was extracted from the clinical samples with the
531 QIAamp® Viral RNA Mini kit (Qiagen, #52904) following the manufacturer's instructions (140µl
532 of swab were extracted and eluted in 60µl). For the validation study (Figure 4), RNA was
533 extracted from 200 µl of the selected gargle and NP specimens with the MagnaPure Compact
534 System (Roche, Penzberg, Germany) using the Nucleic Acid isolation Kit I (Roche) resulting in
535 100 µl of eluate. Residual volume of gargle and NP specimens was stored at 4°C and sent to
536 the DKFZ for further analysis.

537

538 **RT-qPCR**

539 CDC taqman RT-qPCR initially (Figure 1) was performed in technical triplicates according to
540 published protocols⁷⁶, which we adapted to a 384-well plate format and a reduced reaction
541 volume of 12.5 µl. The reaction was performed using the Superscript III One-Step RT-PCR kit
542 with Platinum Taq Polymerase. Magnesium sulphate and BSA were added to the reaction to a
543 final concentration of 0.8 mM and 0.04 µg/µl, respectively. Primers and probes for the viral N1
544 and N2 and the human RNase P genes were added as ready-made mix (1 µl; Integrated DNA
545 Technologies Belgium; CatNo. 10006713). The E-gene probes and primers (GATC, Germany)
546 were used at final concentrations of 500 nM for each primer and 125 nM for the probe. ROX
547 was added to a final concentration of 50 nM. PCR was performed in a QuantStudio 5
548 thermocycler, with cycling conditions 55°C for 10 min, 95°C for 3 min, followed by 45 cycles of
549 95°C for 15 s and 58°C for 30 s.

550

551 For the validation study (Figure 4), real-time PCR of 10 µl RNA-eluate was performed on a
552 BioRad CX96 cycler using the Sarbeco E-Gen-Kit (Fa. Tib Molbiol, Berlin, Germany) following
553 the manufacturer's instructions. Residual volume of extracted RNA from gargle and NP
554 specimens was stored at -20°C and sent to the DKFZ for further analysis.

555

556 **Lysis of clinical samples for direct SARS-CoV-2 detection**

557 Clinical samples were lysed for direct SHERLOCK or ADESSO assay (Figures 2) as follows:
558 after vortexing, 10µl of sample were mixed with 10µl of QuickExtract DNA Extraction solution

559 (Lucigen, #QE09050). In the optimised protocol (Figure 4), QuickExtract DNA Extraction
560 solution is enriched with Rnase Inhibitor, Murine (NEB, #M0314) at a final concentration of
561 4U/μl. Samples were then incubated at 95°C for 5 min. After incubation, samples were mixed by
562 vortexing and spun down for 15 seconds at 10.000g. Finally, 5.6 μl of sample (for RT-RPA 2X)
563 were collected from the upper liquid phase, carefully avoiding to aspirate any precipitate, and
564 used in the RT-RPA step.

565

566 **crRNA synthesis and purification**

567 CRISPR-RNAs (crRNAs) were either designed in our lab or synthesised by Integrated DNA
568 Technologies (IDT). All crRNAs used in this study are listed in **Supplementary File 3**. To
569 produce the crRNAs in our lab we followed a previously published protocol⁵³. In short, the
570 templates for the crRNAs were ordered as DNA oligonucleotides from Sigma-Aldrich with an
571 appended T7 promoter sequence. These oligos were annealed with a T7-3G oligonucleotide,
572 and used in an in vitro transcription (IVT) reaction (HiScribe T7 Quick High Yield RNA Synthesis
573 Kit, NEB, #E2050S). The crRNAs were then purified using Agencourt RNAClean XP Kit
574 (Beckman Coulter, #A63987). The correct size of the crRNAs was confirmed on a UREA gel
575 and the concentration evaluated by nanodrop. Aliquots of 10ng/μl of each crRNA were
576 produced to avoid repeated freeze and thaw cycles and stored at -80°C.

577

578 **Reverse Transcriptase Recombinase polymerase amplification (RT-RPA)**

579 RT-RPA reactions were carried out with TwistAmp Basic (TwistDx, #TABAS03KIT) with the
580 addition of M-MuLV Reverse Transcriptase (NEB, #M0253) and RNase Inhibitor, Murine (NEB,
581 #M0314). Reactions were run at 42°C for 45 minutes in a heat block. Here are the details for the
582 optimised reaction (so called RT-RPA 2X): two lyophilized pellets TwistAmp Basic are used to
583 prepare the following master mix for 5 reactions: 59 μl of Rehydration Buffer (RB) are mixed
584 with 2,5 μl of each primer (forward and reverse) at a concentration of 20μM, 1.5 μl of M-MuLV
585 RetroTranscriptase (200U/μl - NEB, #M0253) and 1,5 μl of Rnase Inhibitor, Murine (40U/μl -
586 NEB, #M0314). The RB-primer-enzyme mix is used to rehydrate two pellets and finally 5μl of
587 MgOAc are added. The complete mix is aliquoted (14.4μl) on top of 5,6 μl of each sample. The
588 RT-RPA protocol was optimised throughout the study. To avoid any confusion, we provide an
589 additional file (**Supplementary File 4**) with detailed protocols for each experiment presented in
590 this work. All RPA primers used in this study are listed in **Supplementary File 3** and were
591 designed following the provided guidelines⁵³.

592

593 **Cas13 cleavage reaction for lateral flow readout**

594 The reaction mix for Cas13 activity was prepared by combining 4.3 μl of nuclease-free water, 1
595 μl of cleavage buffer (400mM Tris pH 7.4), 1 μl of LwaCas13a protein diluted in Storage Buffer
596 (SB)⁵³ to a concentration of 126.6 μg/ml, 0.5 μl of crRNA (40 ng/μl), 0.5 μl of lateral flow reporter
597 (IDT, diluted in water to 20 μM), 0.5 μl of SUPERase-In RNase inhibitor (ThermoFisher
598 Scientific, #AM2694), 0.4 μl of rNTP solution mix (25mM each, NEB, #N0466), 0.3 μl of NxGen
599 T7 RNA Polymerase (Lucigen, #30223-2) and 0.5 μl of MgCl₂ (120mM). 1 μl of the RT-RPA-
600 amplified product was then added to the mix and, after vortexing and spinning down, the mixture
601 was incubated for 10 minutes at 37°C in a heat block. The Cas13 protocol was optimised

602 throughout the study. To avoid any confusion, we provide an additional file (**Supplementary**
603 **File 4**) with detailed protocols for each experiment presented in this work.

604

605 **Lateral flow readout**

606 Lateral flow detection was performed using commercially available detection strips (Milenia
607 HybriDetect 1, TwistDx, Gießen, #MILENIA01). The 10 μ l-LwaCas13a reactions were transferred
608 to a tube already containing 80 μ l of HybriDetect Assay buffer. After vortexing and spinning
609 down the reaction mix, a lateral flow dipstick was added to the reaction tube. The result was
610 clearly readable after one minute. Once the whole reaction volume was absorbed, the dipstick
611 was removed and photographed with a smartphone camera for band intensity quantification
612 performed with the freely available ImageJ image processing program⁷⁷. The results are shown
613 as intensity ratio (test band/control band) and test were considered positive for value of intensity
614 ratio above 0.2 based on the results shown in Figure S3.

615

616 **Cas13 cleavage reaction for fluorescence readout**

617 The reaction mix for Cas13 activity was prepared by combining 8.6 μ l of nuclease-free water, 2
618 μ l of cleavage buffer (400mM Tris pH 7.4), 2 μ l of LwaCas13a protein diluted in Storage Buffer
619 (SB) to a concentration of 126.6 μ g/ml, 1 μ l of crRNA (40ng/ μ l), 1 μ l of fluorescent reporter (IDT,
620 diluted in water to a final concentration of 4 μ M), 1 μ l of RNase inhibitor, Murine (NEB, #M0314),
621 0.8 μ l of rNTP solution mix (25mM each, NEB, #N0466), 0.6 μ l of NxGen T7 RNA Polymerase
622 (Lucigen, #30223-2) and 1 μ l of MgCl₂ (120mM). 2 μ l of the RT-RPA-amplified product was
623 then added to the mix. The 20 μ l-LwaCas13a reactions were transferred in 5 μ l-replicates (4
624 wells each sample) to a 384-well, round, black-well, clear-bottom plate (Corning, #3544). The
625 plate was briefly spun down at 500g for 15 sec to remove potential bubbles and placed into a
626 pre-heated GloMax® Explorer plate reader (Promega) at 37°C.

627

628 **Fluorescence readout**

629 Fluorescence was measured every 5 min for 3 h. Data analysis, if not otherwise stated, was
630 performed at the 30-min time-point.

631

632 **RNase activity detection assay**

633 In order to check for RNase activity in clinical samples, 10 μ l of a negative swab and gargle
634 water sample (Figure 2) were mixed with 10 μ l of QuickExtract DNA Extraction Solution with or
635 without RNase Inhibitor, Murine (NEB, M0314) at a final concentration of 4U/ μ l. The samples
636 were then incubated at 95°C for 5 min. After incubation, RNaseAlert substrate v2 (RNaseAlert
637 Lab Test Kit v2, #4479768, Thermo Fisher Scientific) was added at a final concentration of
638 200nM. The samples were mixed by vortexing, spun down and incubated at RT for 30 min in the
639 dark. After incubation, the samples were transferred to a 384-well, round, black-well, clear-
640 bottom plate (Corning, #3544) in 5 μ l-replicates (4 wells each sample). The plate was briefly
641 spun down at 500g for 15 sec to remove potential bubbles and placed into a GloMax Explorer
642 plate reader (Promega). RNaseAlert substrate fluorescence was measured every 5 min for 30
643 min. Data analysis, if not differently stated, was performed at the 5-min time-point.

644

645 **ACKNOWLEDGEMENTS**

646

647 We thank the transport service staff, German Cancer Research Center (DKFZ), for providing
648 excellent transportation services of all the clinical samples from the Medical University
649 Mannheim to the DKFZ. The work was supported by a grant from the Ministry of Science,
650 Research and the Arts of Baden-Württemberg for COVID-19 research (grant agreement no.
651 Kap. 1499 TG 93 to Dr. Riccardo Pecori, Prof. Dr. Nina Papavasiliou (DKFZ) and Prof. Dr.
652 Thomas Miethke (Medical Faculty of Mannheim)). Several schematics presented here were
653 created with Biorender.com.

654

655 **AUTHOR CONTRIBUTIONS**

656

657 BC, RP, and FNP designed the experiments. JPV and AH produced Cas13 protein. BC and RP
658 performed all the experiments using SHERLOCK/ADESSO. PB and BR performed confirmative
659 RT-qPCR on clinical samples using CDC protocol. MK collected the specimens and AGK
660 performed the RT-qPCR on clinical samples using Tib Molbiol, under the supervision of SW. SA
661 quantified the bands of the lateral flow strips. BC and RP analyzed the data and wrote the
662 manuscript. RP, TM and FNP conceived the study and supervised the research. All authors
663 have read and approved the manuscript.

664

665

666 **COMPETING INTERESTS**

667

668 The DKFZ has filed patent applications regarding this diagnostic methodology (EP 20 173
669 912.5). RP, FNP and BC are inventors on the above-mentioned patent applications.

670

671

672 **REFERENCES**

673

674 1. WHO Coronavirus (COVID-19) Dashboard. <https://covid19.who.int>.

675 2. Zhu, N. *et al.* A Novel Coronavirus from Patients with Pneumonia in China, 2019. *N. Engl. J.*

676 *Med.* **382**, 727–733 (2020).

677 3. Huang, C. *et al.* Clinical features of patients infected with 2019 novel coronavirus in Wuhan,

678 China. *The Lancet* **395**, 497–506 (2020).

679 4. Gorbalenya, A. E. *et al.* The species Severe acute respiratory syndrome-related coronavirus:

680 classifying 2019-nCoV and naming it SARS-CoV-2. *Nat. Microbiol.* **5**, 536–544 (2020).

681 5. Cevik, M. *et al.* SARS-CoV-2, SARS-CoV, and MERS-CoV viral load dynamics, duration of

682 viral shedding, and infectiousness: a systematic review and meta-analysis. *Lancet Microbe* **2**,

683 e13–e22 (2021).

- 684 6. Backer, J. A., Klinkenberg, D. & Wallinga, J. Incubation period of 2019 novel coronavirus
685 (2019-nCoV) infections among travellers from Wuhan, China, 20–28 January 2020.
686 *Eurosurveillance* **25**, (2020).
- 687 7. Lauer, S. A. *et al.* The Incubation Period of Coronavirus Disease 2019 (COVID-19) From
688 Publicly Reported Confirmed Cases: Estimation and Application. *Ann. Intern. Med.* **172**, 577–
689 582 (2020).
- 690 8. Wölfel, R. *et al.* Virological assessment of hospitalized patients with COVID-2019. *Nature*
691 **581**, 465–469 (2020).
- 692 9. To, K. K.-W. *et al.* Temporal profiles of viral load in posterior oropharyngeal saliva samples
693 and serum antibody responses during infection by SARS-CoV-2: an observational cohort
694 study. *Lancet Infect. Dis.* **20**, 565–574 (2020).
- 695 10. Salvatore, P. P. *et al.* Epidemiological Correlates of Polymerase Chain Reaction Cycle
696 Threshold Values in the Detection of Severe Acute Respiratory Syndrome Coronavirus 2
697 (SARS-CoV-2). *Clin. Infect. Dis.* ciaa1469 (2020) doi:10.1093/cid/ciaa1469.
- 698 11. Singanayagam, A. *et al.* Duration of infectiousness and correlation with RT-PCR cycle
699 threshold values in cases of COVID-19, England, January to May 2020. *Eurosurveillance* **25**,
700 (2020).
- 701 12. Ferretti, L. *et al.* Quantifying SARS-CoV-2 transmission suggests epidemic control with
702 digital contact tracing. *Science* **368**, eabb6936 (2020).
- 703 13. Lavezzo, E. *et al.* Suppression of a SARS-CoV-2 outbreak in the Italian municipality of
704 Vo'. *Nature* **584**, 425–429 (2020).
- 705 14. Gudbjartsson, D. F. *et al.* Spread of SARS-CoV-2 in the Icelandic Population. *N. Engl. J.*
706 *Med.* **382**, 2302–2315 (2020).
- 707 15. Bai, Y. *et al.* Presumed Asymptomatic Carrier Transmission of COVID-19. (2020).
- 708 16. Rothe, C. *et al.* Transmission of 2019-nCoV Infection from an Asymptomatic Contact in
709 Germany. *N. Engl. J. Med.* **382**, 970–971 (2020).

- 710 17. Chan, J. F.-W. *et al.* A familial cluster of pneumonia associated with the 2019 novel
711 coronavirus indicating person-to-person transmission: a study of a family cluster. *The Lancet*
712 **395**, 514–523 (2020).
- 713 18. Day, M. Covid-19: four fifths of cases are asymptomatic, China figures indicate. *BMJ*
714 m1375 (2020) doi:10.1136/bmj.m1375.
- 715 19. Sahin, U. *et al.* COVID-19 vaccine BNT162b1 elicits human antibody and TH1 T cell
716 responses. *Nature* **586**, 594–599 (2020).
- 717 20. Sahin, U. *et al.* BNT162b2 induces SARS-CoV-2-neutralising antibodies and T cells in
718 humans. <http://medrxiv.org/lookup/doi/10.1101/2020.12.09.20245175> (2020)
719 doi:10.1101/2020.12.09.20245175.
- 720 21. Anderson, E. J. *et al.* Safety and Immunogenicity of SARS-CoV-2 mRNA-1273 Vaccine
721 in Older Adults. *N. Engl. J. Med.* **383**, 2427–2438 (2020).
- 722 22. Voysey, M. *et al.* Safety and efficacy of the ChAdOx1 nCoV-19 vaccine (AZD1222)
723 against SARS-CoV-2: an interim analysis of four randomised controlled trials in Brazil, South
724 Africa, and the UK. *The Lancet* **397**, 99–111 (2021).
- 725 23. COVID-19 vaccines. *European Vaccination Information Portal* [https://vaccination-](https://vaccination-info.eu/en/covid-19/covid-19-vaccines)
726 [info.eu/en/covid-19/covid-19-vaccines](https://vaccination-info.eu/en/covid-19/covid-19-vaccines).
- 727 24. About covid19-projections.com. *COVID-19 Projections Using Machine Learning*
728 <https://covid19-projections.com/about/>.
- 729 25. Vokó, Z. & Pitter, J. G. The effect of social distance measures on COVID-19 epidemics
730 in Europe: an interrupted time series analysis. *GeroScience* **42**, 1075–1082 (2020).
- 731 26. Roberts, L. How COVID hurt the fight against other dangerous diseases. *Nature* **592**,
732 502–504 (2021).
- 733 27. Nicola, M. *et al.* The socio-economic implications of the coronavirus pandemic (COVID-
734 19): A review. *Int. J. Surg.* **78**, 185–193 (2020).
- 735 28. Maringe, C. *et al.* The impact of the COVID-19 pandemic on cancer deaths due to

- 736 delays in diagnosis in England, UK: a national, population-based, modelling study. *Lancet*
737 *Oncol.* **21**, 1023–1034 (2020).
- 738 29. Donthu, N. & Gustafsson, A. Effects of COVID-19 on business and research. *J. Bus.*
739 *Res.* **117**, 284–289 (2020).
- 740 30. Larremore, D. B. *et al.* Test sensitivity is secondary to frequency and turnaround time for
741 COVID-19 screening. *Sci. Adv.* **7**, eabd5393 (2021).
- 742 31. Vogels, C. B. F. *et al.* Analytical sensitivity and efficiency comparisons of SARS-CoV-2
743 RT-qPCR primer–probe sets. *Nat. Microbiol.* **5**, 1299–1305 (2020).
- 744 32. Dinnes, J. *et al.* Rapid, point-of-care antigen and molecular-based tests for diagnosis of
745 SARS-CoV-2 infection. *Cochrane Database Syst. Rev.* (2021)
746 doi:10.1002/14651858.CD013705.pub2.
- 747 33. Abudayyeh, O. O. & Gootenberg, J. S. CRISPR diagnostics. *Science* **372**, 914–915
748 (2021).
- 749 34. Abudayyeh, O. O. *et al.* C2c2 is a single-component programmable RNA-guided RNA-
750 targeting CRISPR effector. *Science* **353**, aaf5573 (2016).
- 751 35. Chen, Y. *et al.* N1-Methyladenosine detection with CRISPR-Cas13a/C2c2. *Chem. Sci.*
752 **10**, 2975–2979 (2019).
- 753 36. East-Seletsky, A., O’Connell, M. R., Burstein, D., Knott, G. J. & Doudna, J. A. RNA
754 Targeting by Functionally Orthogonal Type VI-A CRISPR-Cas Enzymes. *Mol. Cell* **66**, 373-
755 383.e3 (2017).
- 756 37. Notomi, T. Loop-mediated isothermal amplification of DNA. *Nucleic Acids Res.* **28**, 63e–
757 663 (2000).
- 758 38. Piepenburg, O., Williams, C. H., Stemple, D. L. & Armes, N. A. DNA Detection Using
759 Recombination Proteins. *PLoS Biol.* **4**, e204 (2006).
- 760 39. Gootenberg, J. S. *et al.* Nucleic acid detection with CRISPR-Cas13a/C2c2. *Science* **356**,
761 438–442 (2017).

- 762 40. Gootenberg, J. S. *et al.* Multiplexed and portable nucleic acid detection platform with
763 Cas13, Cas12a, and Csm6. *Science* **360**, 439–444 (2018).
- 764 41. Jung, J. *et al.* Point-of-care testing for COVID-19 using SHERLOCK diagnostics.
765 <http://medrxiv.org/lookup/doi/10.1101/2020.05.04.20091231> (2020)
766 doi:10.1101/2020.05.04.20091231.
- 767 42. Broughton, J. P. *et al.* CRISPR–Cas12-based detection of SARS-CoV-2. *Nat.*
768 *Biotechnol.* **38**, 870–874 (2020).
- 769 43. Arizti-Sanz, J. *et al.* Streamlined inactivation, amplification, and Cas13-based detection
770 of SARS-CoV-2. *Nat. Commun.* **11**, 5921 (2020).
- 771 44. Brandsma, E. *et al.* Rapid, Sensitive, and Specific Severe Acute Respiratory Syndrome
772 Coronavirus 2 Detection: A Multicenter Comparison Between Standard Quantitative Reverse-
773 Transcriptase Polymerase Chain Reaction and CRISPR-Based DETECTR. *J. Infect. Dis.*
774 **223**, 206–213 (2021).
- 775 45. Huang, Z. *et al.* Ultra-sensitive and high-throughput CRISPR-powered COVID-19
776 diagnosis. *Biosens. Bioelectron.* **164**, 112316 (2020).
- 777 46. Patchesung, M. *et al.* Clinical validation of a Cas13-based assay for the detection of
778 SARS-CoV-2 RNA. *Nat. Biomed. Eng.* **4**, 1140–1149 (2020).
- 779 47. Rauch, J. N. *et al.* A Scalable, Easy-to-Deploy Protocol for Cas13-Based Detection of
780 SARS-CoV-2 Genetic Material. *J. Clin. Microbiol.* **59**, 8 (2021).
- 781 48. Fozouni, P. *et al.* Amplification-free detection of SARS-CoV-2 with CRISPR-Cas13a and
782 mobile phone microscopy. *Cell* **184**, 323-333.e9 (2021).
- 783 49. FDA. Letter of Authorization for Sherlock CRISPR SARS-CoV-2 Kit. (2020).
- 784 50. FDA. Letter of Authorization for SARS-CoV-2 RNA DETECTR Assay. (2020).
- 785 51. Bullard, J. *et al.* Predicting Infectious Severe Acute Respiratory Syndrome Coronavirus 2
786 From Diagnostic Samples. *Clin. Infect. Dis.* **71**, 2663–2666 (2020).
- 787 52. Agrawal, A. India's COVID crisis flags need to forecast variants. *Nature* **594**, 9–9 (2021).

- 788 53. Kellner, M. J., Koob, J. G., Gootenberg, J. S., Abudayyeh, O. O. & Zhang, F.
789 SHERLOCK: nucleic acid detection with CRISPR nucleases. *Nat. Protoc.* **14**, 2986–3012
790 (2019).
- 791 54. Zhang, F., Abudayyeh, O. O. & Gootenberg, J. S. A protocol for detection of COVID-19
792 using CRISPR diagnostics. (2020).
- 793 55. Qian, J. *et al.* An enhanced isothermal amplification assay for viral detection. *Nat.*
794 *Commun.* **11**, 5920 (2020).
- 795 56. CDC. CDC 2019-nCoV Real-Time RT-PCR Diagnostic Panel Instructions for Use.
796 (2020).
- 797 57. Fomsgaard, A. S. & Rosenstjerne, M. W. An alternative workflow for molecular detection
798 of SARS-CoV-2 – escape from the NA extraction kit-shortage, Copenhagen, Denmark, March
799 2020. *Eurosurveillance* **25**, (2020).
- 800 58. Akst, J. RNA Extraction Kits for COVID-19 Tests Are in Short Supply in US. *The*
801 *Scientist Magazine*@ [https://www.the-scientist.com/news-opinion/rna-extraction-kits-for-covid-](https://www.the-scientist.com/news-opinion/rna-extraction-kits-for-covid-19-tests-are-in-short-supply-in-us-67250)
802 [19-tests-are-in-short-supply-in-us-67250](https://www.the-scientist.com/news-opinion/rna-extraction-kits-for-covid-19-tests-are-in-short-supply-in-us-67250) (2020).
- 803 59. Smyrlaki, I. *et al.* Massive and rapid COVID-19 testing is feasible by extraction-free
804 SARS-CoV-2 RT-PCR. *Nat. Commun.* **11**, 4812 (2020).
- 805 60. Bruce, E. A. *et al.* Direct RT-qPCR detection of SARS-CoV-2 RNA from patient
806 nasopharyngeal swabs without an RNA extraction step. *PLOS Biol.* **18**, e3000896 (2020).
- 807 61. Metsky, H. C., Freije, C. A., Kosoko-Thoroddsen, T.-S. F., Sabeti, P. C. & Myhrvold, C.
808 *CRISPR-based surveillance for COVID-19 using genomically-comprehensive machine*
809 *learning design*. <http://biorxiv.org/lookup/doi/10.1101/2020.02.26.967026> (2020)
810 doi:10.1101/2020.02.26.967026.
- 811 62. Korber, B. *et al.* Tracking Changes in SARS-CoV-2 Spike: Evidence that D614G
812 Increases Infectivity of the COVID-19 Virus. *Cell* **182**, 812-827.e19 (2020).
- 813 63. Davies, N. G. *et al.* Estimated transmissibility and impact of SARS-CoV-2 lineage

- 814 B.1.1.7 in England. *Science* **372**, eabg3055 (2021).
- 815 64. Davies, N. G. *et al.* Increased mortality in community-tested cases of SARS-CoV-2
816 lineage B.1.1.7. *Nature* **593**, 270–274 (2021).
- 817 65. Tegally, H. *et al.* Detection of a SARS-CoV-2 variant of concern in South Africa. *Nature*
818 **592**, 438–443 (2021).
- 819 66. Pearson, C. A. B. *et al.* Estimates of severity and transmissibility of novel South Africa
820 SARS-CoV-2 variant 501Y.V2. (2021).
- 821 67. Wang, P. *et al.* Antibody resistance of SARS-CoV-2 variants B.1.351 and B.1.1.7.
822 *Nature* **593**, 130–135 (2021).
- 823 68. Madhi, S. A. *et al.* Efficacy of the ChAdOx1 nCoV-19 Covid-19 Vaccine against the
824 B.1.351 Variant. *N. Engl. J. Med.* **384**, 1885–1898 (2021).
- 825 69. Abu-Raddad, L. J., Chemaitelly, H. & Butt, A. A. Effectiveness of the BNT162b2 Covid-
826 19 Vaccine against the B.1.1.7 and B.1.351 Variants. *N. Engl. J. Med.* NEJMc2104974
827 (2021) doi:10.1056/NEJMc2104974.
- 828 70. Byrne, R. L. *et al.* Saliva Alternative to Upper Respiratory Swabs for SARS-CoV-2
829 Diagnosis. *Emerg. Infect. Dis.* **26**, 2769–2770 (2020).
- 830 71. Ott, I. M. *et al.* *Simply saliva: stability of SARS-CoV-2 detection negates the need for*
831 *expensive collection devices*. <http://medrxiv.org/lookup/doi/10.1101/2020.08.03.20165233>
832 (2020) doi:10.1101/2020.08.03.20165233.
- 833 72. Lindner, A. K. *et al.* SARS-CoV-2 patient self-testing with an antigen-detecting rapid test:
834 a head-to-head comparison with professional testing. (2021)
835 doi:10.1101/2021.01.06.20249009.
- 836 73. Aleta, A. *et al.* Modelling the impact of testing, contact tracing and household quarantine
837 on second waves of COVID-19. *Nat. Hum. Behav.* **4**, 964–971 (2020).
- 838 74. Gettleman, J., Yasir, S., Kumar, H., Raj, S. & Loke, A. As Covid-19 Devastates India,
839 Deaths Go Undercounted. *The New York Times* (2021).

- 840 75. Reagent calculator for portal. [https://www.who.int/publications/m/item/reagent-calculator-](https://www.who.int/publications/m/item/reagent-calculator-for-portal)
841 for-portal.
- 842 76. Corman, V. M. *et al.* Detection of 2019 novel coronavirus (2019-nCoV) by real-time RT-
843 PCR. *Eurosurveillance* **25**, (2020).
- 844 77. ImageJ. <https://imagej.net/Welcome>.

845
846
847
848

849 FIGURE LEGENDS

850

851 **Figure 1: A SHERLOCK-based assay for SARS-CoV-2 detection in clinical samples. A.**
852 Graphic of SHERLOCK experimental workflow to detect SARS-CoV-2 in RNA extracted from
853 clinical samples with lateral flow readout. **B.** SHERLOCK sensitivity on serial dilutions of an IVT
854 fragment of SARS-CoV-2 S and Orf1a genes. **C.** Comparison of SARS-CoV-2 detection on RNA
855 extracted from 30 clinical samples via SHERLOCK and RT-qPCR (Medical University Hospital
856 Mannheim (RT-qPCR hospital) or CDC 2019-nCoV Real-Time RT-PCR Diagnostic Panel).
857 SHERLOCK was performed on SARS-CoV-2 S gene; RT-qPCR at the Medical University
858 Hospital Mannheim was performed on SARS-CoV-2 E and Orf1a genes; CDC RT-qPCR was
859 performed on SARS-CoV-2 N1, N2 and E genes (CDC N1, N2, E) and human RNase P (CDC
860 Rp) as RNA quality control. T = test band; C = control band; nd = not detected; NTC = non
861 template control.

862

863 **Figure 2: SARS-CoV-2 direct detection from clinical samples. A.** Graphic of SHERLOCK
864 experimental workflow to detect SARS-CoV-2 in unextracted clinical samples with lateral flow
865 readout. **B.** Comparison of three lysis methods for direct detection of SARS-CoV-2 in a COVID-
866 19 positive clinical sample (sample #30 in Figure 1C) via SHERLOCK with lateral flow readout.
867 Each lysis method was performed in triplicates. **C.** Determination of SHERLOCK sensitivity with
868 lateral flow readout on serial dilutions of SARS-CoV-2 synthetic genome spiked in a negative
869 sample lysed with QuickExtract DNA Extraction Solution. For **B-C** band intensity ratios are
870 shown in the bar plots on the right. T = test band; C = control band; NTC = non template control.
871 **D.** SHERLOCK performance on 160 unextracted clinical samples with lateral flow readout. Only
872 the band intensity ratios of the COVID-19 positive samples (n = 93) are shown in the bar plot.
873 LoD = Limit of Detection. **E.** Concordance between SHERLOCK (on unextracted samples) and
874 RT-qPCR (on extracted RNA) for 160 clinical samples (93 positive and 67 negative).

875

876 **Figure 3: ADESSO: an optimised and highly sensitive SHERLOCK assay. A.** Measurement
877 of RNase activity in a swab sample lysed at 95°C for 5 minutes with QuickExtract DNA
878 Extraction Solution enriched or not with RNase inhibitor, Murine, at a final concentration of 4
879 U/μl. **B.** Comparison of SHERLOCK sensitivity on serial dilutions of SARS-CoV-2 genome with

880 different reverse transcriptases in presence or absence of RNase H. **C.** Optimisation of
881 SHERLOCK sensitivity with lateral flow readout by increasing the RPA reagents to detect a
882 false negative sample (#L151, **Supplementary File 1**). A true negative sample (#L126,
883 **Supplementary File 1**) is used as negative control. The lateral flow strips whose band intensity
884 ratios are plotted here are shown in Figure S4B. 1xRPA corresponds to the standard amount of
885 RPA described in the original SHERLOCK protocol⁵³ and 5xRPA corresponds to the optimal
886 amount recommended by the manufacturer. **D.** Confirmation of the improved SHERLOCK
887 sensitivity with 2xRPA compared to 1xRPA on clinical samples with Ct values close to our LoD
888 based on Figure 2 (**Supplementary File 1**). The lateral flow strips whose band intensity ratios
889 are plotted here are shown in Figure S4C. **E.** Optimisation of the Cas13 reaction kinetics by
890 increasing the amount of Cas13 protein and crRNA in the reaction with fluorescence readout.
891 The reaction kinetics is evaluated by measuring the fluorescence signal at different time-points.
892 The complete 3-hour analysis is shown in Figure S4D. **F.** Time-point analysis of the optimised
893 Cas13 reaction in half the volume to determine the shortest incubation time required to detect a
894 positive signal with lateral flow readout. The lateral flow strips whose band intensity ratios are
895 plotted here are shown in Figure S4E. **G.** Sensitivity of the improved SHERLOCK protocol with
896 lateral flow readout on serial dilutions of SARS-CoV-2 synthetic genome upon integration of all
897 the above-described optimisations. Intensity ratios are shown in the bar plot on the right. T =
898 test band; C = control band. **H.** Graphic of the experimental workflow of ADESSO to detect
899 SARS-CoV-2 in unextracted clinical samples with lateral flow or fluorescence readout.

900
901 **Figure 4: Evaluation of ADESSO performance on clinical samples in direct comparison to**
902 **RT-qPCR. A.** Schematic of the validation study to assess ADESSO performance for SARS-
903 CoV-2 detection in clinical samples in comparison with RT-qPCR (Tib Molbiol). The COVID-19
904 status of the samples included in the study was initially determined by RT-qPCR (COBAS).
905 ADESSO was performed on both extracted RNA and unextracted samples with lateral flow
906 readout. The results interpretation for ADESSO was performed without knowledge of the
907 outcome of RT-qPCR. **B.** ADESSO performance on RNA extracted from swab specimens in
908 comparison with COBAS RT-qPCR. Negative samples by Tib Molbiol RT-qPCR are represented
909 in orange. **C.** ADESSO performance on unextracted swab specimens in comparison with
910 COBAS RT-qPCR (performed on RNA extracted from swabs). **D.** ADESSO performance on
911 RNA extracted from gargle (G) samples in comparison with COBAS RT-qPCR (performed on
912 RNA extracted from swabs). Negative samples by Tib Molbiol RT-qPCR are represented in
913 pink. **E.** ADESSO performance on unextracted G samples in comparison with COBAS RT-
914 qPCR (performed on RNA extracted from swabs). Samples missed by ADESSO with low Ct
915 values (<28) according to COBAS RT-qPCR on RNA extracted from swabs but high Ct values
916 according to Tib Molbiol RT-qPCR on RNA extracted from G samples are represented in dark
917 red. **F.** Correlation analysis of Ct values obtained with Tib Molbiol RT-qPCR (y axis) or COBAS
918 RT-qPCR (x axis) on RNA extracted from swab specimens. Negative samples by Tib Molbiol
919 RT-qPCR are represented in orange and are excluded in the calculation of the correlation (R).
920 **G.** Correlation analysis of Ct values obtained with Tib Molbiol RT-qPCR (y axis) and COBAS
921 RT-qPCR (x axis) on RNA extracted from G samples. Negative samples by Tib Molbiol RT-
922 qPCR are represented in pink and are excluded in the calculation of the correlation (R). **H.**
923 Correlation analysis of Ct values obtained after Tib Molbiol RT-qPCR on RNA extracted from G

924 (y axis) and swab (x axis) samples. Negative swab samples are represented in orange; negative
925 G samples are represented in pink; negative samples both as G and swab are represented in
926 red. All the negative samples are excluded in the calculation of the correlation (R). Samples
927 missed by ADESSO with low Ct values (<28) according to COBAS RT-qPCR on RNA extracted
928 from swabs but high Ct values according to Tib Molbiol RT-qPCR on RNA extracted from G
929 samples are represented in dark red. For panels **B, C, D, E** only the band intensity ratios of the
930 positive samples are shown (n = 95). Values higher than 1 are plotted as equal to 1 for better
931 visualisation. LoD = Limit of detection.

932

933 **Figure 5: Adaptation of ADESSO for detection of SARS-CoV-2 variants: a flexible and**
934 **powerful assay to rapidly identify specific variants or mutations. A.** Schematic of SARS-
935 CoV-2 S gene with annotation of the reported mutations for SARS-CoV-2 B.1.1.7 (top) and
936 B.1.351 (bottom) lineages. The regions of the S gene targeted by ADESSO and ADESSO-UK
937 are indicated in purple and orange, respectively. **B.** Schematic of the S gene region containing
938 the Δ HV69-70 deletion (highlighted in pink) specific for the B.1.1.7 variant in comparison with
939 the original SARS-CoV-2 sequence from Wuhan and illustration of the binding of the specific
940 crRNAs targeting the mutated (crRNA Δ HV69-70) or Wuhan (crRNA HV69-70) sequence. The
941 grey sequence in the crRNAs is called direct repeat (DR) and its stem-loop structure is needed
942 for the recruitment of Cas13. **C.** SARS-CoV-2 detection by ADESSO in 13 clinical samples
943 carrying either the UK (B.1.1.7) or SA (B.1.351) SARS-CoV-2 variant. The band intensity ratios
944 are shown in the bar plot on the right. **D.** SARS-CoV-2 B.1.1.7 variant detection by ADESSO-UK
945 with Δ HV69-70 crRNA and **(E)** confirmation of the presence of SARS-CoV-2 B.1.351 variant by
946 ADESSO-UK with HV69-70 crRNA in the same samples. For **C, D, E**, T = test band; C = control
947 band; NTC = non template control. **F.** Schematic of the binding of the forward RPA primer used
948 in ADESSO to the complementary region in the original SARS-CoV-2 sequence from Wuhan
949 (top), in clinical samples #12 and #13 carrying the SA variant with the deletion Δ 242-244
950 (middle) and in sample #11 carrying the SA variant with an additional mutation (R246I) that
951 disrupts the primer binding (bottom). The positions of the Δ 242-244 deletion and the R246I
952 mutation are highlighted in grey. The point mutation causing the R246I substitution is marked in
953 red.

954

955

956 SUPPLEMENTARY FIGURE LEGENDS

957

958 **Figure S1: Generation of LwaCas13a and first attempt of SHERLOCK. A.** LwaCas13a
959 protein purification. The LwaCas13 fusion construct also encodes multiple affinity tags and a
960 protease recognition site at the N terminus of the polypeptide. We have utilized the 6xHIS tag as
961 the basis for our relatively inexpensive purification, while others have developed an alternative
962 protocol based on the Strep-tags⁵³. After expression in Rosetta cells (inducible via the Lac
963 operon), the cells are lysed by sonication and the nucleic acid contained within the lysate is
964 digested. The fusion protein is then purified by nickel-affinity chromatography. The purified
965 fusion protein is digested with SUMO protease, which cleaves the tags and majority of the
966 SUMO site off of the mature protein. The SUMO protease and in-tact affinity tags are then
967 removed from the sample by re-applying the sample to the nickel column, leaving >98% pure

968 Cas13. We also employ a size exclusion chromatography step to remove any aggregated
969 Cas13 protein (not pictured). **B.** Serially diluted amounts of pure Cas13 were analyzed by
970 coomassie staining after conventional SDS-PAGE, revealing a prominent band at the
971 appropriate molecular weight and only minor contaminants. A serial dilution of BSA was also run
972 as an estimate of protein concentration by densitometry (which was also validated by BCA
973 assay). **C.** Sensitivity of home-made Cas13 on serial dilutions of an in-vitro-transcribed (IVT)
974 fragment of SARS-CoV-2 S gene in the absence of pre-amplification step. Comparison between
975 fully purified fresh Cas13, partially purified fresh SUMO-Cas13 and fully purified Cas13 stored
976 overnight (o.n.) at 4°C. Both the band intensity ratios (top) and the corresponding lateral flow
977 strips (bottom) are shown. **D.** Comparison of SHERLOCK sensitivity on the same IVT fragment
978 as in panel C when using either ProtoScript II Retro-Transcriptase (as previously published⁵⁴) or
979 M-MuLV Retro-Transcriptase in the RT-RPA step.

980
981 **Figure S2: SHERLOCK optimisation: input amount and test of different sets of primers-**
982 **crRNA. A.** Determination of SHERLOCK sensitivity on serial dilution of SARS-CoV-2 synthetic
983 genome upon optimisation of RT units and RNA input in the RT-RPA reaction with lateral flow
984 readout. **B.** Comparison of SHERLOCK performance on different genes in SARS-CoV-2
985 genome by using alternative sets of primers-crRNA targeting N2 (version 1 and version 2),
986 Orf1a⁶¹ and S genes on dilutions of a COVID-19 positive sample (sample #6 in Figure 1C). **C.**
987 Determination of SHERLOCK sensitivity on serial dilutions of SARS-CoV-2 synthetic genome by
988 using the two most sensitive sets of primers-crRNA selected in panel B targeting Orf1a⁶¹ and S
989 genes. For panels **A, B, C**, T = test band; C = control band. For panels **A, C**, NTC = non
990 template control.

991
992 **Figure S3: SARS-CoV-2 clinical samples. Definition of threshold between positive and**
993 **negative results. A.** The bar plot shows the band intensity ratios of all the negative controls
994 utilised in this study (282, in blue) together with the negative (67(Fig. 2) + 100*4(Fig. 4) = 467, in
995 green) and positive (93(Fig. 2) + 95*4(Fig. 4) = 473, in pink) clinical samples analysed in
996 Figures 2 and 4. These data were used to define a threshold band intensity ratio of 0.2 to
997 distinguish between positive and negative samples.

998
999 **Figure S4: ADESSO: an optimised and highly sensitive SHERLOCK assay. A.** Graphic of
1000 SHERLOCK experimental workflow to detect SARS-CoV-2 in unextracted clinical samples with
1001 both lateral flow and fluorescence readout. **B.** Optimisation of SHERLOCK sensitivity with lateral
1002 flow readout by increasing the RPA reagents to detect a false negative sample (#L151,
1003 **Supplementary File 1**). The band intensity ratios of the lateral flow strips shown here are
1004 plotted in Figure 3C. 1xRPA corresponds to the standard amount of RPA described in the
1005 original SHERLOCK protocol⁵³ and 5xRPA corresponds to the optimal amount recommended
1006 by the manufacturer. **C.** Confirmation of the improved SHERLOCK sensitivity with 2xRPA
1007 compared to 1xRPA on clinical samples with Ct values close to the LoD from Figure 2
1008 (**Supplementary File 1**). The band intensity ratios of the lateral flow strips shown here are
1009 plotted in Figure 3D. **D.** Scheme of the experiment and complete measurement of the
1010 fluorescence whose results are shown in Figure 3E. **E.** Time-point analysis of the Cas13
1011 reaction to determine the shortest incubation time required to detect a positive signal with lateral

1012 flow readout. The band intensity ratios of the lateral flow strips shown here are plotted in Figure
1013 3F.

1014
1015 **Figure S5: Adaptation of ADESSO for detection of SARS-CoV-2 variants. A.** RPA primers
1016 optimisation to amplify the region of SARS-CoV-2 S gene surrounding the B.1.1.7 variant-
1017 specific deletion causing Δ HV69-70. Two combinations of the same forward primer with two
1018 alternative reverse primers were tested (set 1 and set 2) on serial dilutions of SARS-CoV-2
1019 synthetic genome (Wuhan sequence). Cas13 detection was performed using crRNA HV69-70.
1020 Band intensity ratios are shown on the right side. T = test band; C = control band. **B.** Band
1021 intensity ratios of 13 clinical samples carrying either the UK (B.1.1.7) or SA (B.1.351) SARS-
1022 CoV-2 variant tested by ADESSO-UK. The corresponding lateral flow strips are shown in Figure
1023 5D and E. The bar plot on the left illustrates the results of the SARS-CoV-2 B.1.1.7 variant
1024 detection by ADESSO-UK with crRNA Δ HV69-70. The bar plot on the right illustrates the results
1025 of the confirmation of the presence of SARS-CoV-2 B.1.351 variant by ADESSO-UK with crRNA
1026 HV69-70. NTC = non template control. **C.** Schematic of SARS-CoV-2 S gene with annotation of
1027 the mutations identified in three patients (clinical samples #11, #12 and #13) carrying the SA
1028 variant. The regions of the S gene targeted by ADESSO and ADESSO-UK are indicated in
1029 purple and orange, respectively. The presence of the mutation R246I in sample #11, here
1030 highlighted in red, disrupts the binding of the RPA forward primer used in ADESSO, thus
1031 impeding the amplification of this region and leading to a false negative result.

1032
1033 **Figure S6: SARS-CoV-2 clinical samples. Frequency distribution of Ct values across the**
1034 **infected patients included in the study. A and B.** Frequency distribution and cumulative
1035 frequency distribution, respectively, of the Ct values of all the positive swab samples analysed in
1036 this work ($n = 211$, **Supplementary File 1**). For both distributions, the bin width is equal to 2
1037 and the R-squared (R^2) was calculated for a gaussian distribution.

1038
1039
1040 **SUPPLEMENTARY MATERIALS**
1041

SHERLOCK on RNA	number			number/total number (percentage)			
	Positive samples (N=10)	Negative samples (N=20)	Total samples (N=30)	Positive predictive value	Negative predictive value	Sensitivity	Specificity
Positive	10	0	10	10/10 (100%)		10/10 (100%)	
Negative	0	20	20		20/20 (100%)		20/20 (100%)

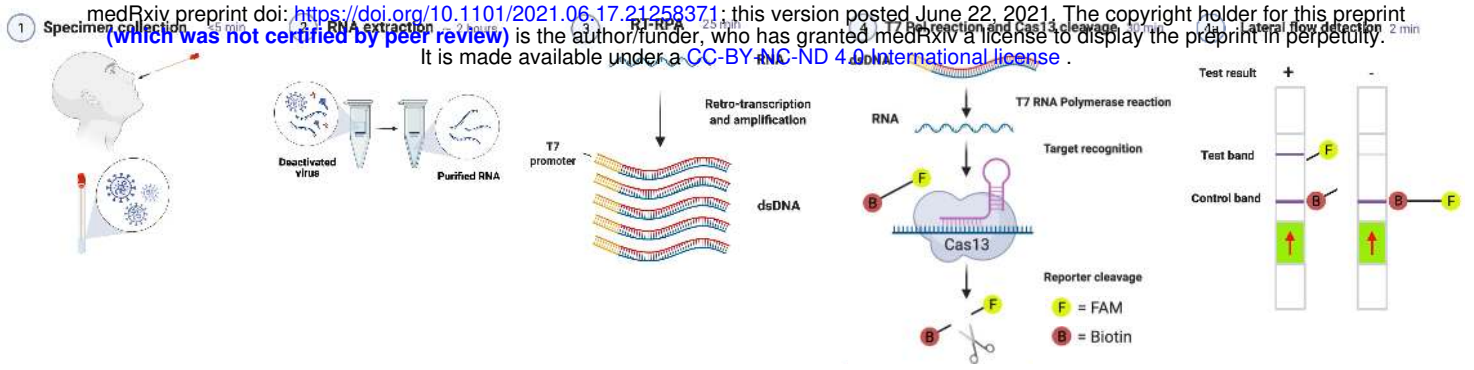
SHERLOCK on unextracted samples	number			number/total number (percentage)			
	Positive samples (N=93)	Negative samples (N=67)	Total samples (N=160)	Positive predictive value	Negative predictive value	Sensitivity	Specificity
Positive	73	0	73	73/73 (100%)		73/93 (78%)	
Negative	20	67	87		67/87 (77%)		67/67 (100%)

1042

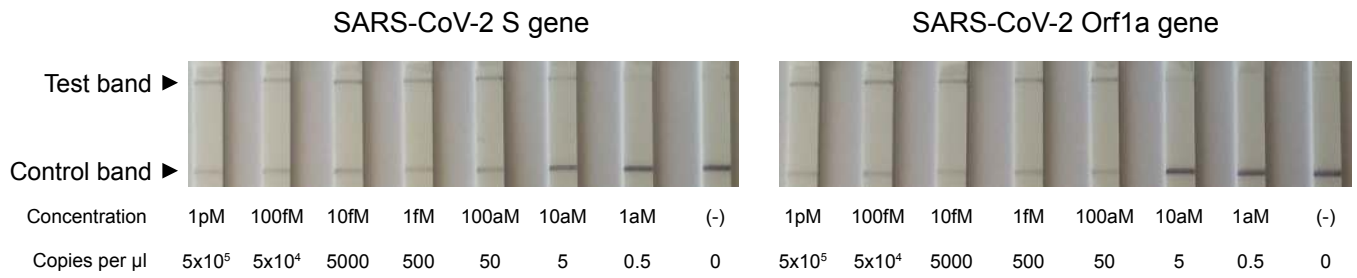
1043 **Table S1:** Positive and negative predictive values, sensitivity and specificity of SHERLOCK on
1044 swab samples with (top) and without (bottom) RNA extraction.

Figure 1

A



B



C

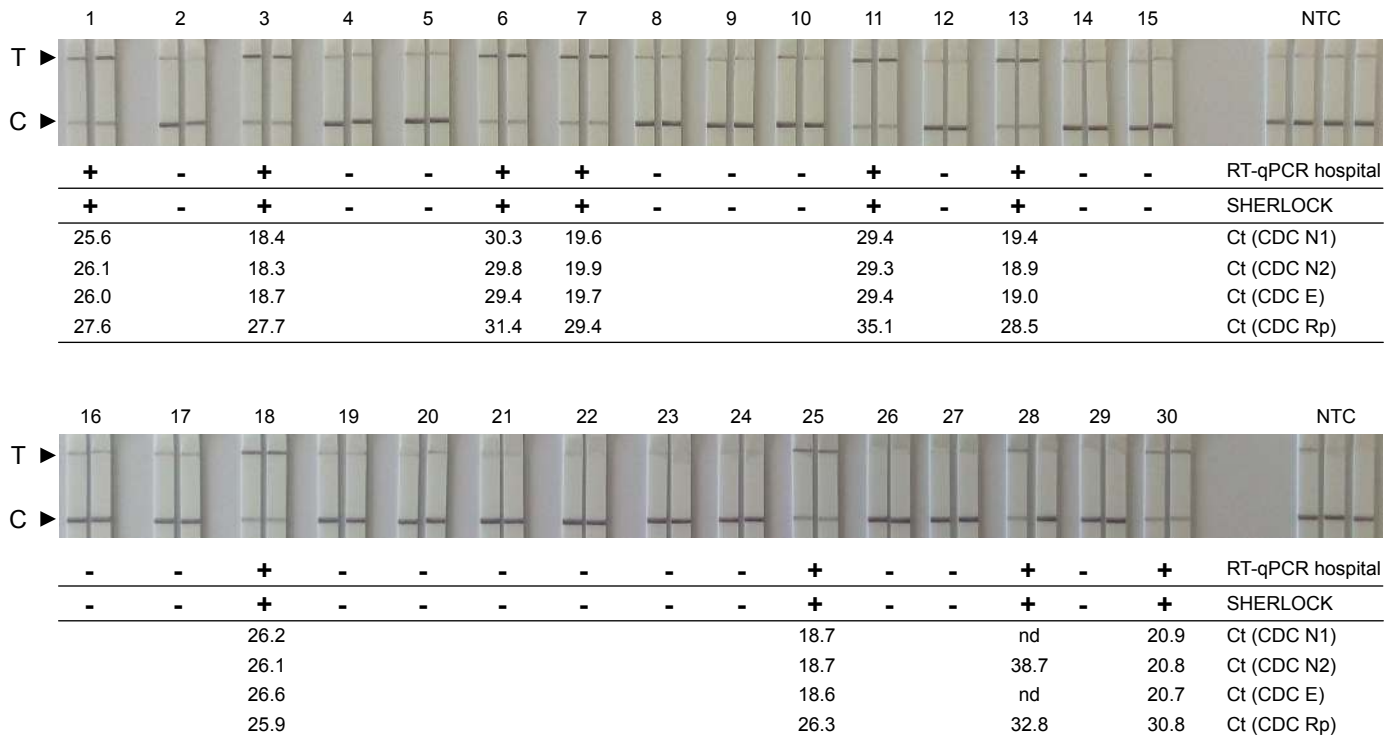
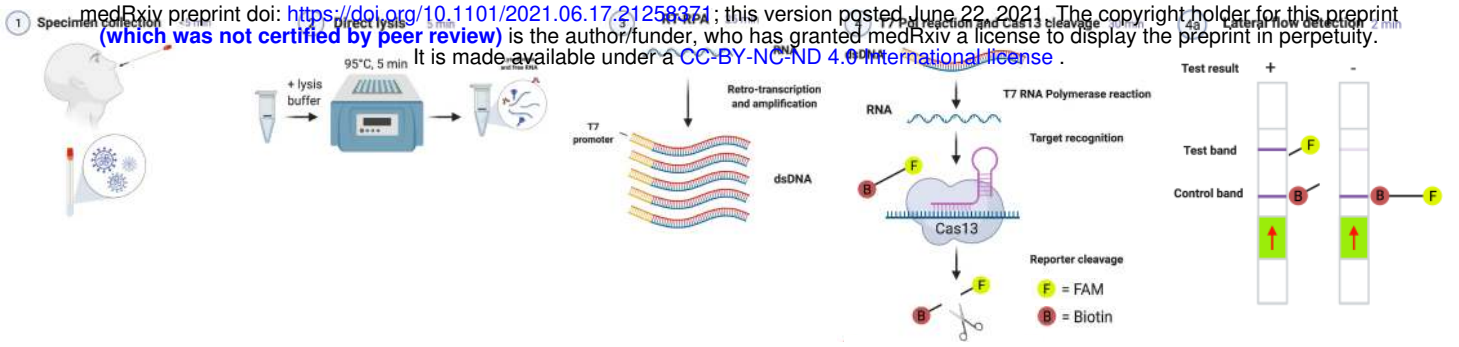
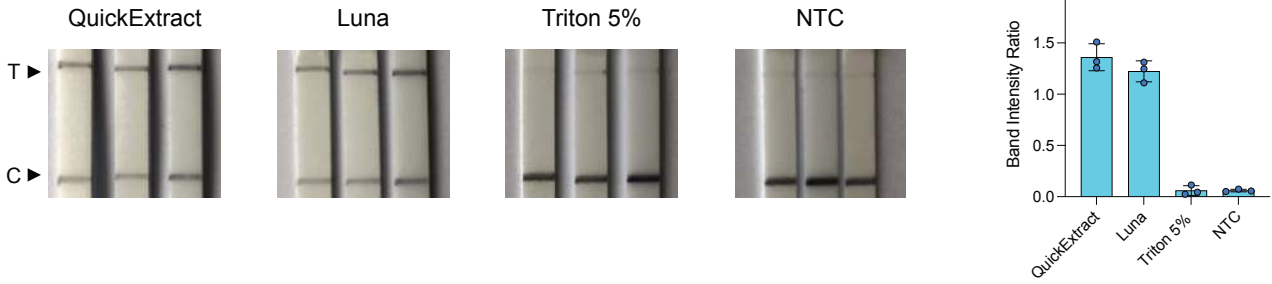


Figure 2

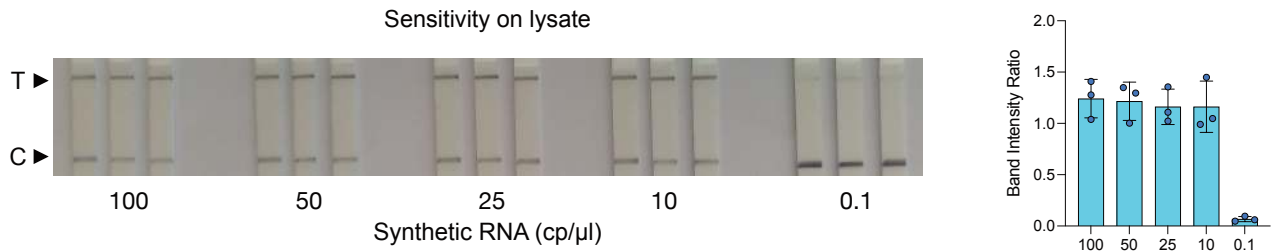
A



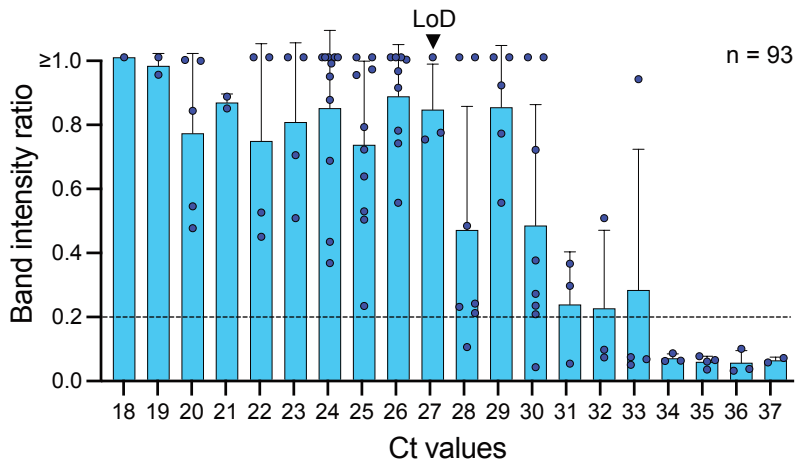
B



C



D



E

		RT-qPCR (RNA)	
		+	-
SHERLOCK (lysate)	+	73	0
	-	20	67

Figure 3

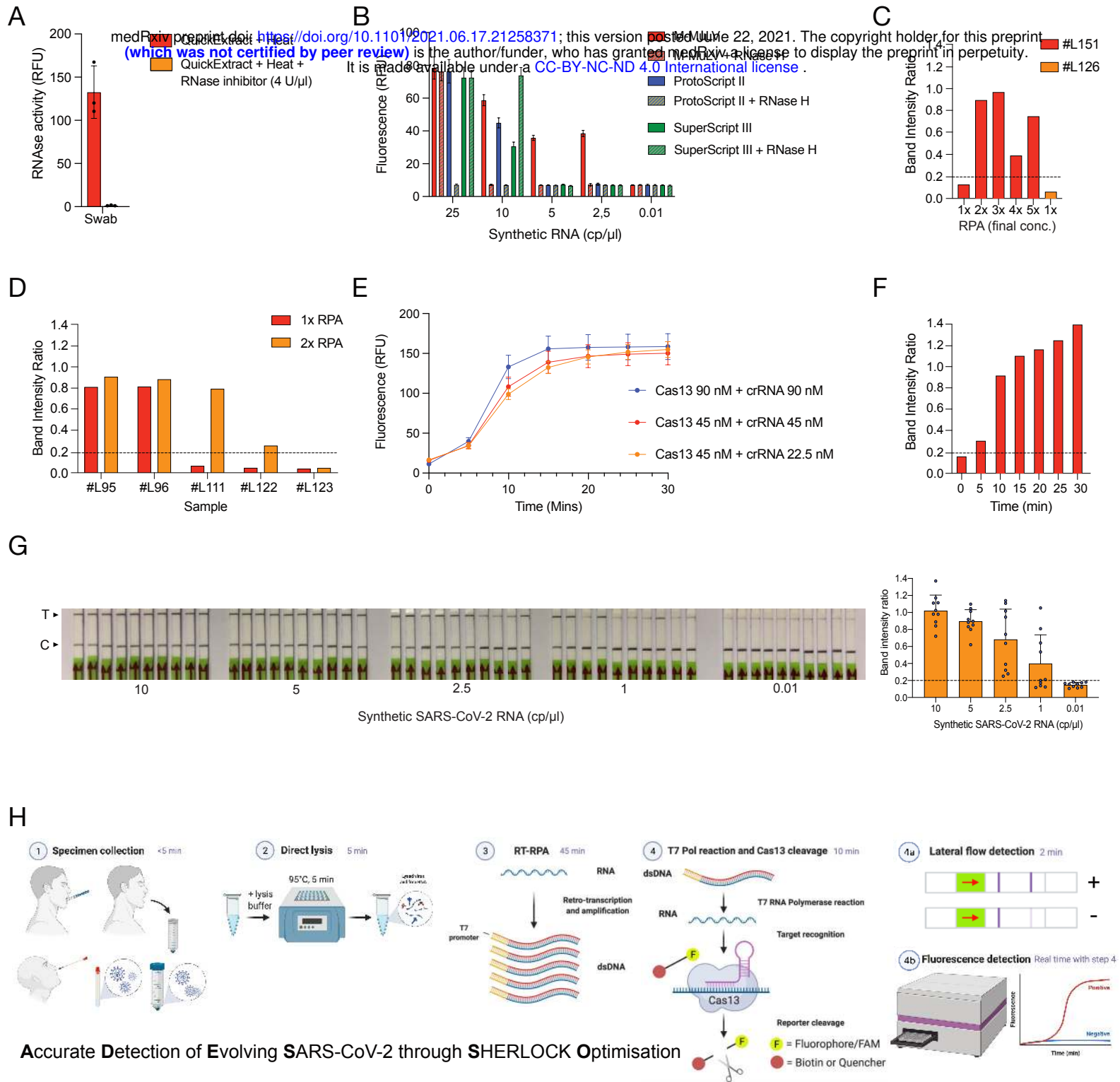


Figure 4

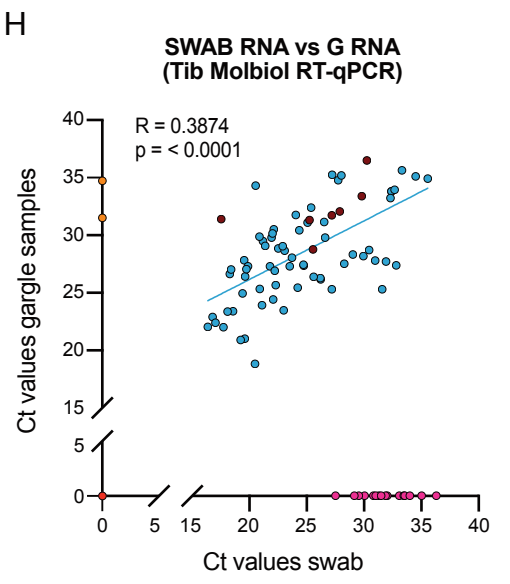
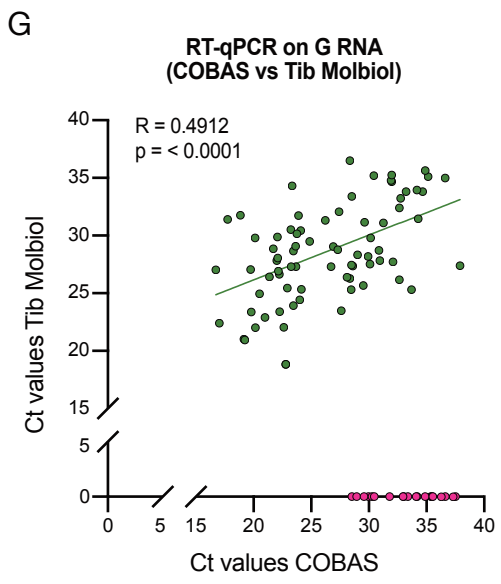
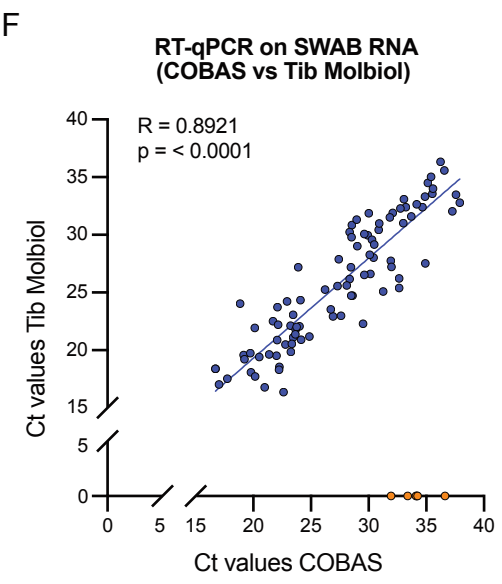
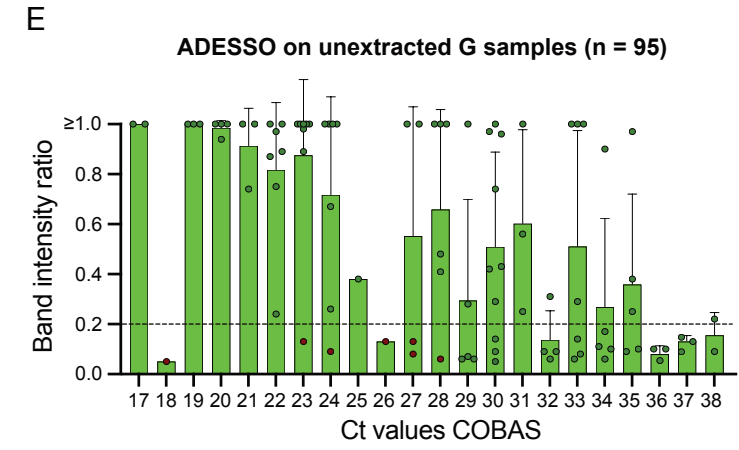
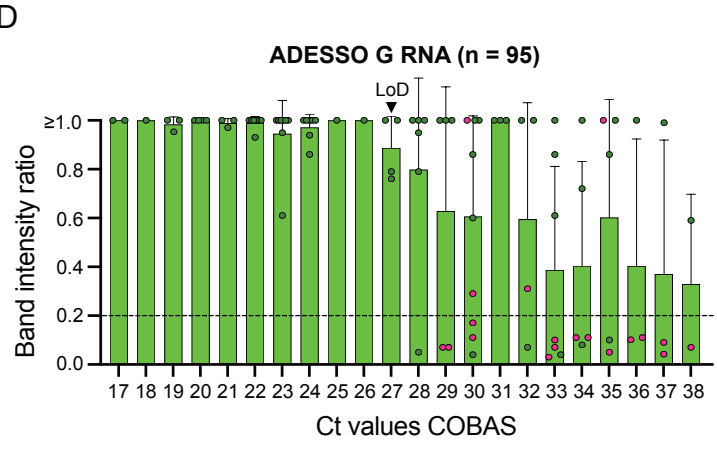
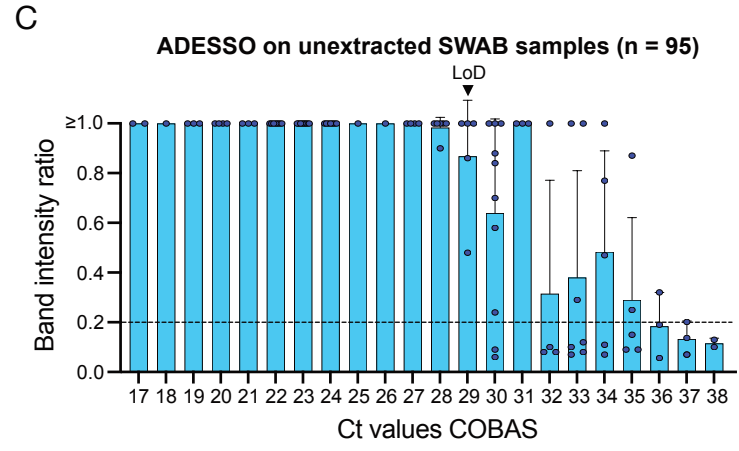
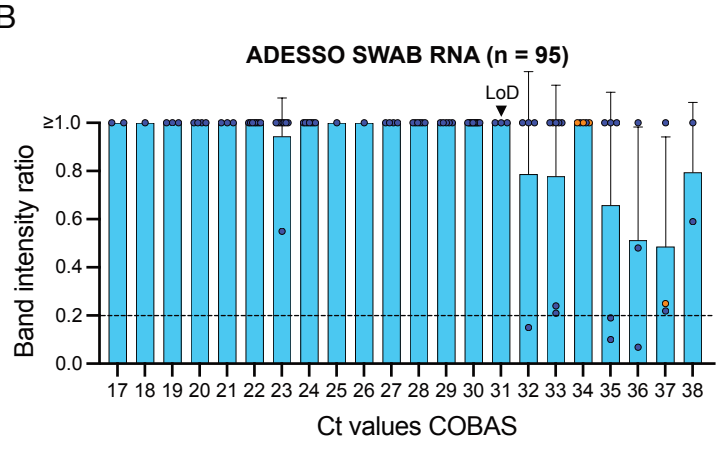
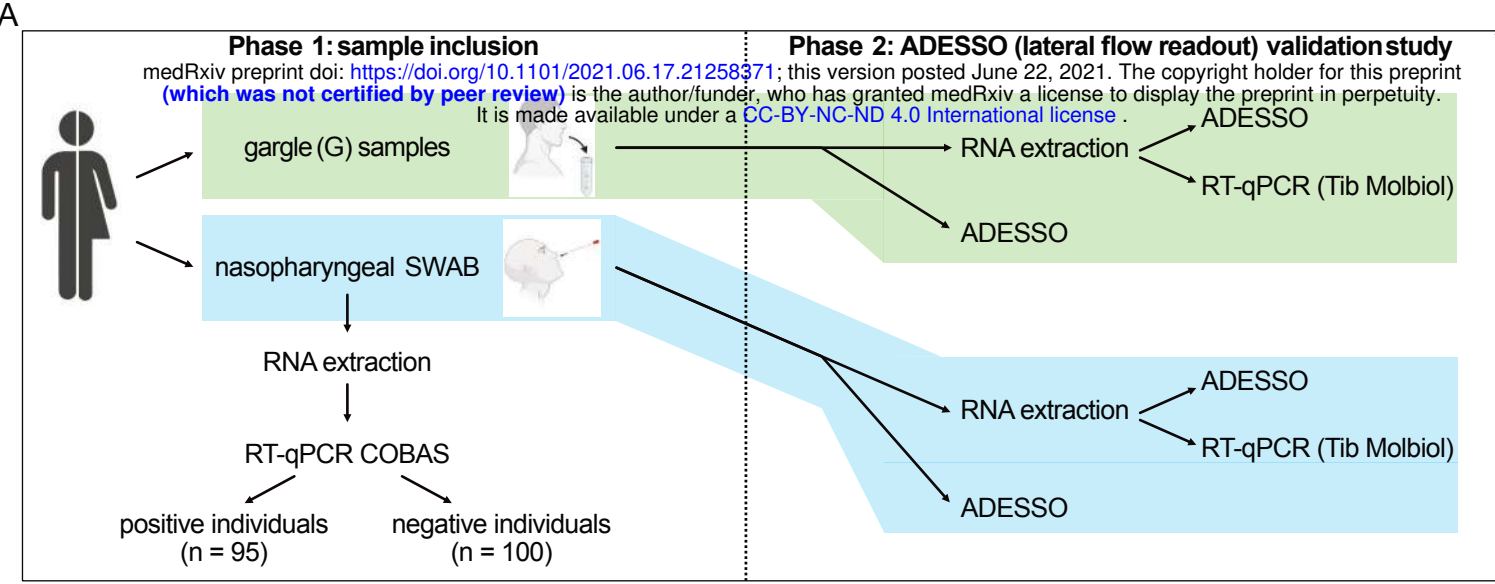
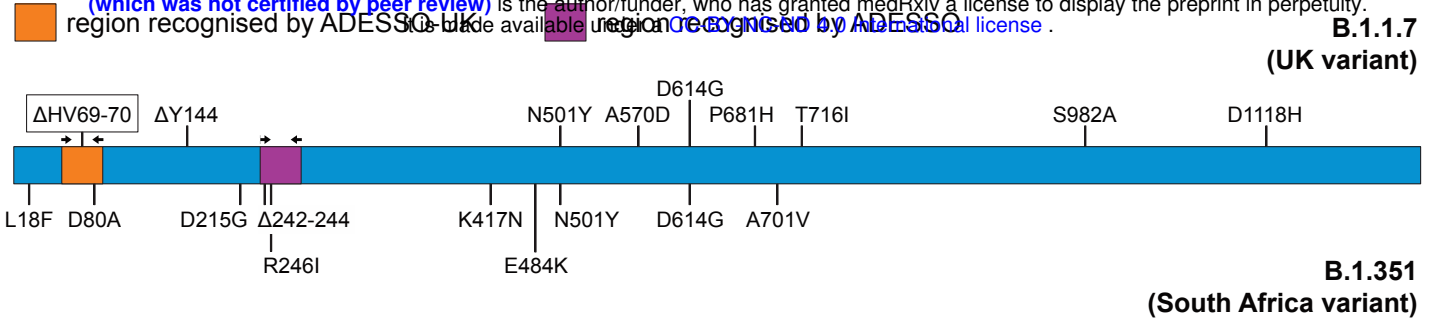


Figure 5

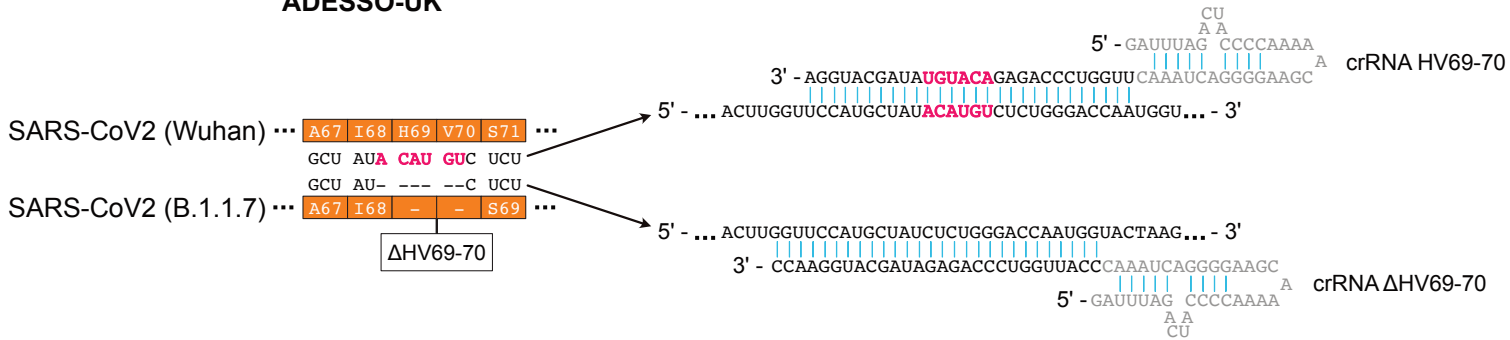
A

medRxiv preprint doi: <https://doi.org/10.1101/2021.06.17.21258371>; this version posted June 22, 2021. The copyright holder for this preprint (which was not certified by peer review) is the author/funder, who has granted medRxiv a license to display the preprint in perpetuity. It is made available under aCC-BY 4.0 International license.



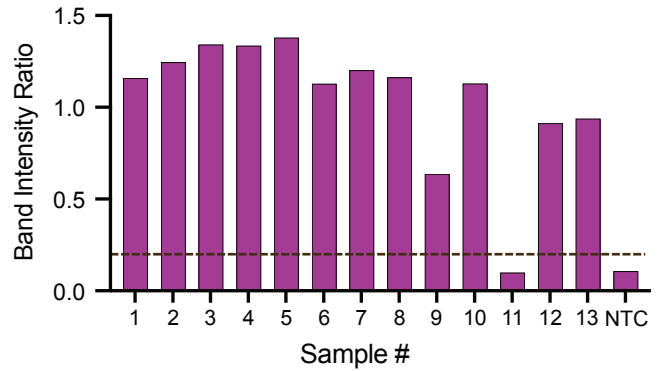
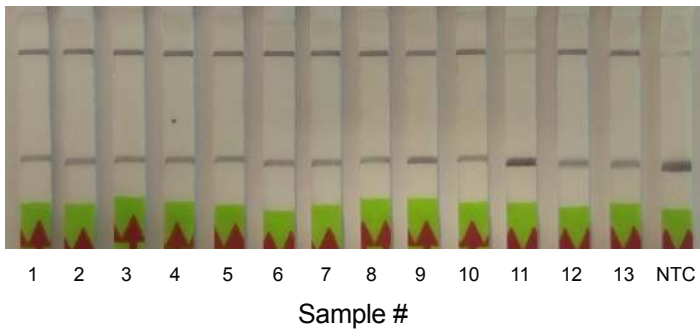
B

ADESSO-UK



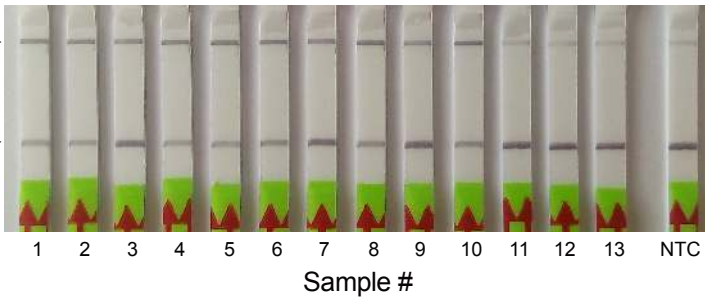
C

ADESSO



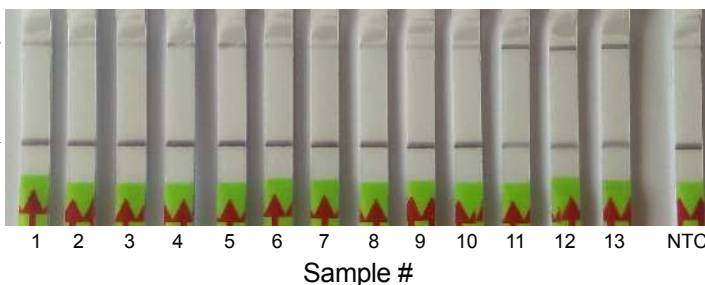
D

ADESSO-UK (crRNA ΔHV69-70)



E

ADESSO-UK (crRNA HV69-70)



F

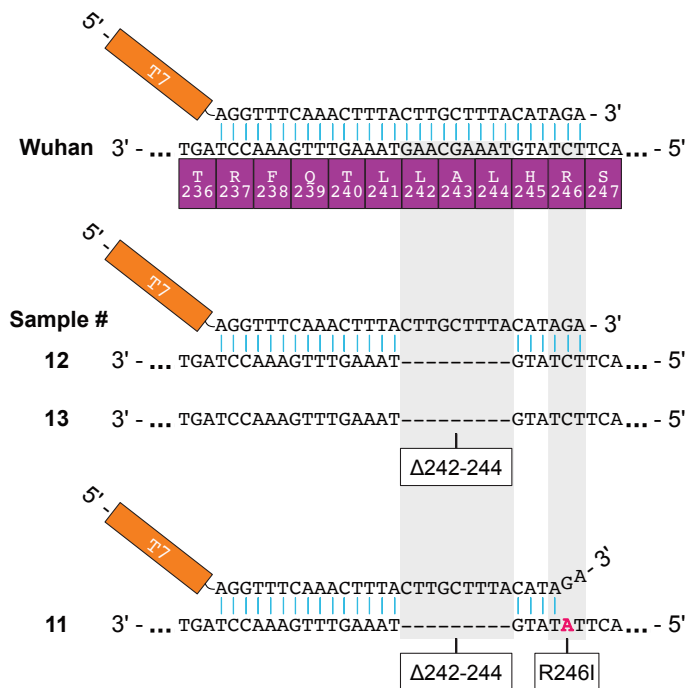
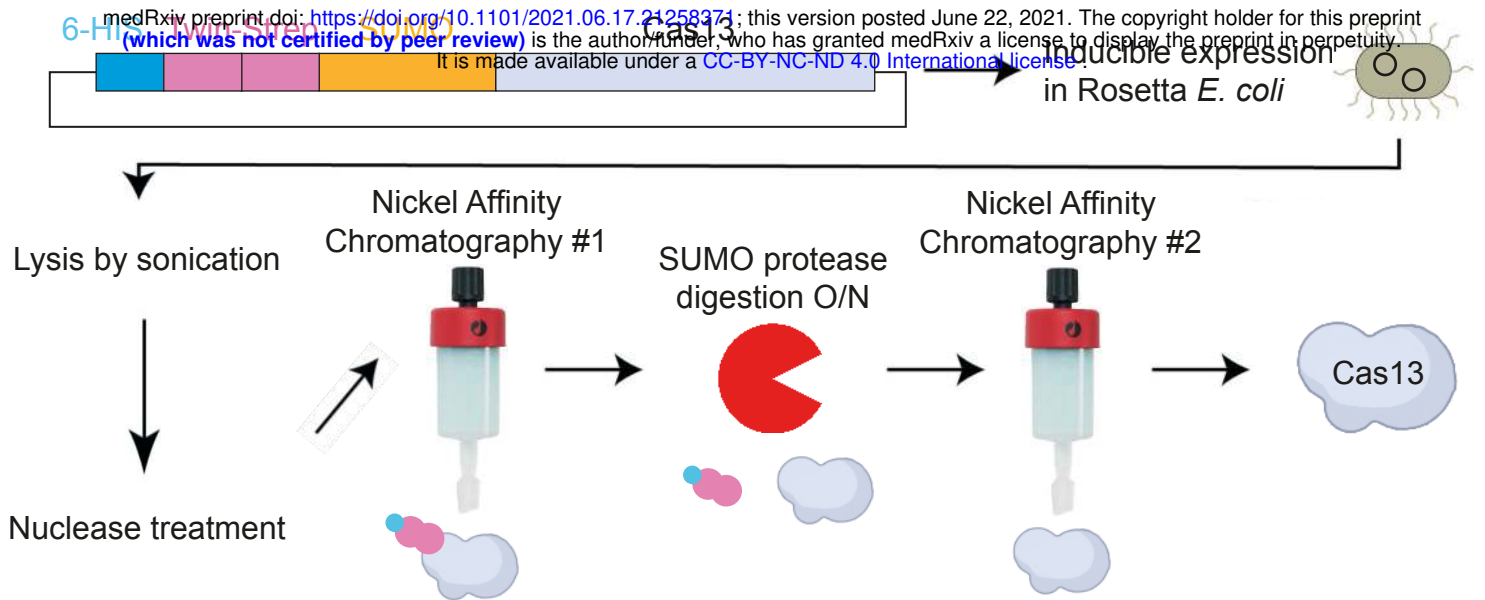
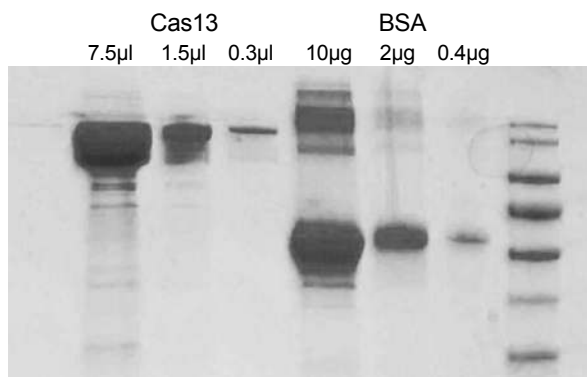


Figure S1

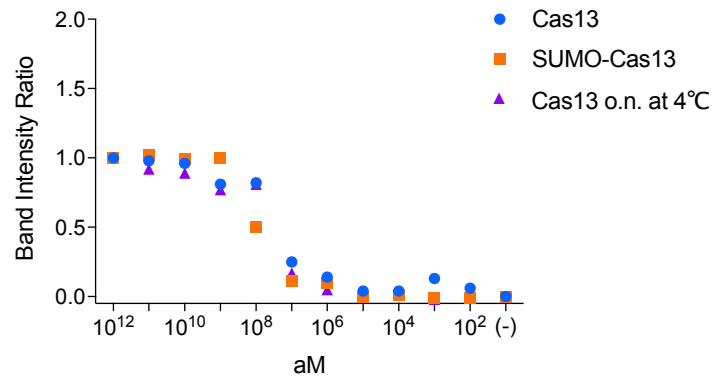
A



B



C



D

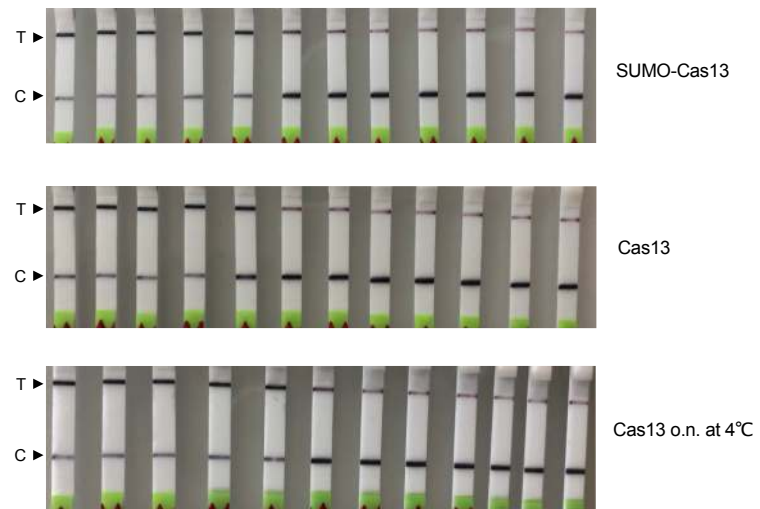
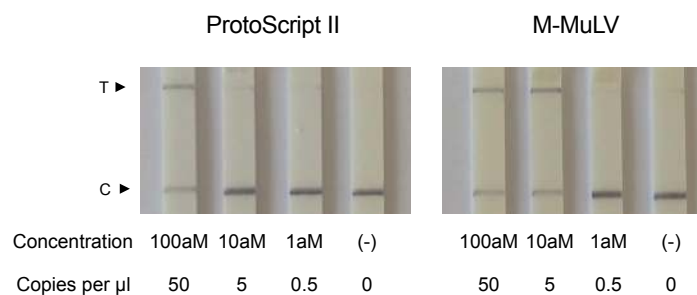
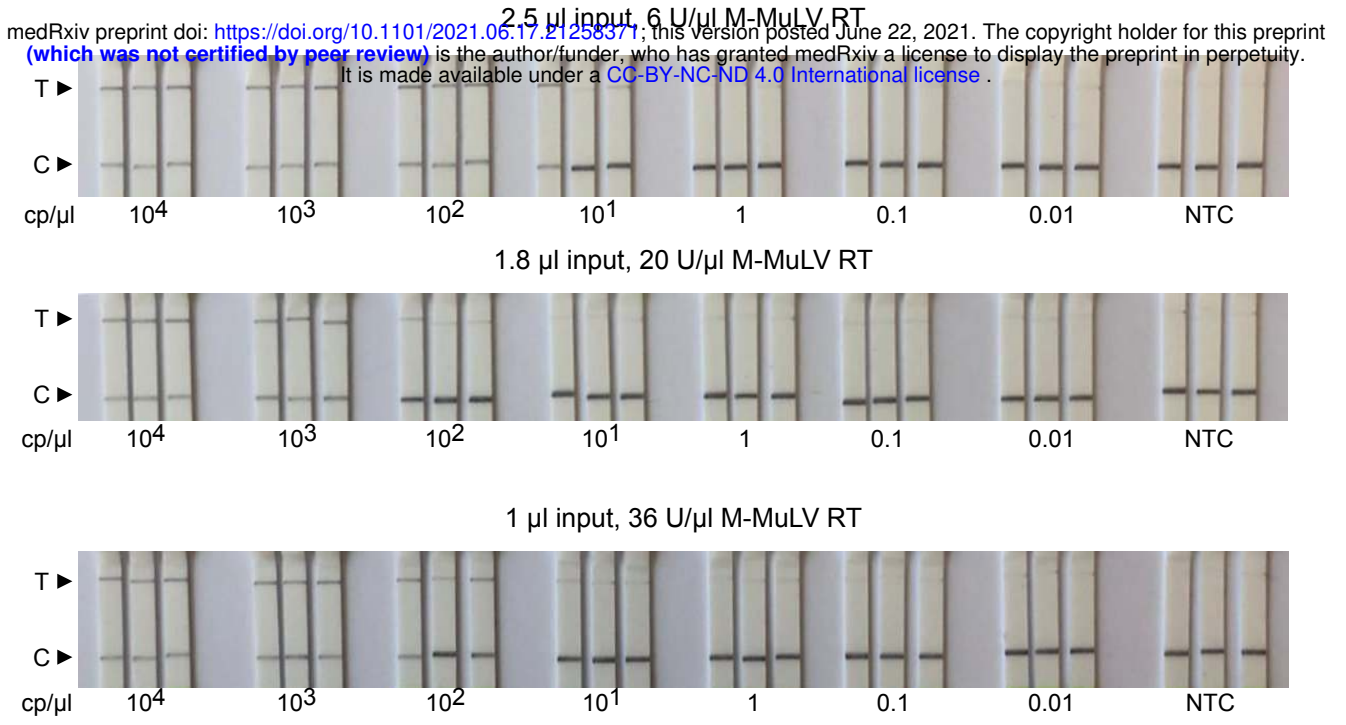
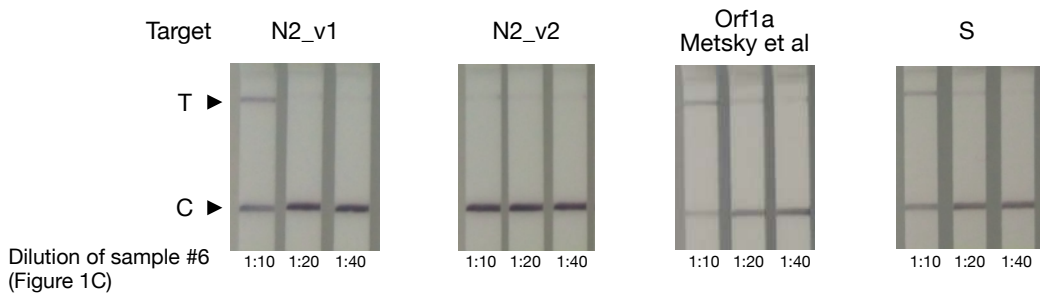


Figure S2

A



B



C

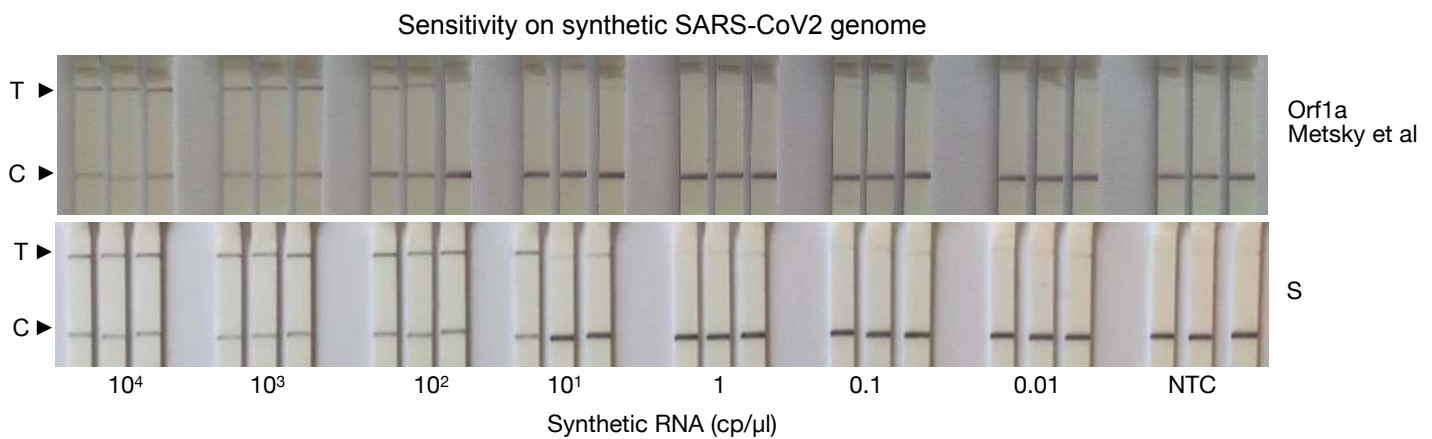


Figure S3

A

medRxiv preprint doi: <https://doi.org/10.1101/2021.06.17.21258371>; this version posted June 22, 2021. The copyright holder for this preprint (which was not certified by peer review) is the author/funder, who has granted medRxiv a license to display the preprint in perpetuity. It is made available under a [CC-BY-NC-ND 4.0 International license](#).

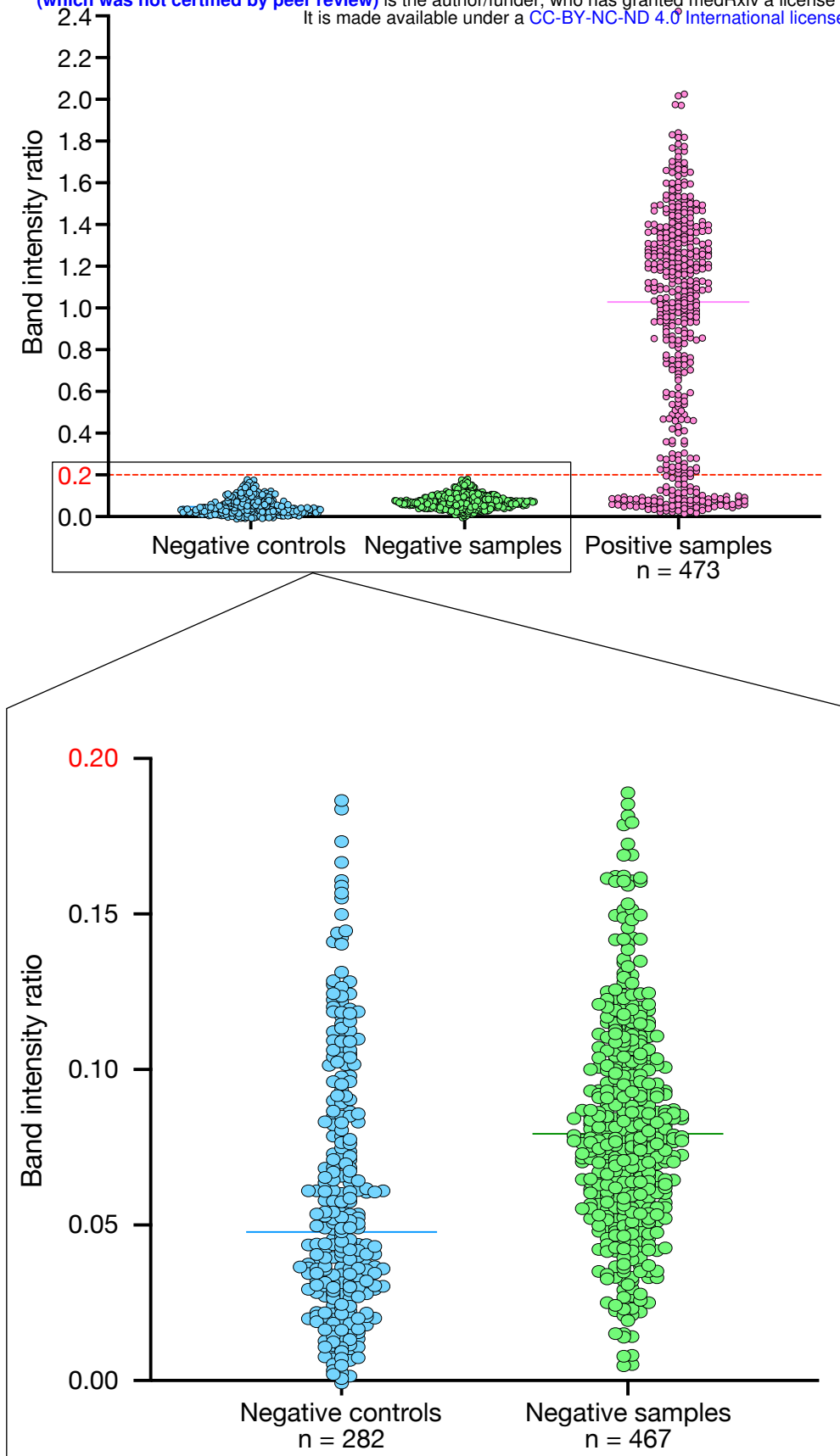
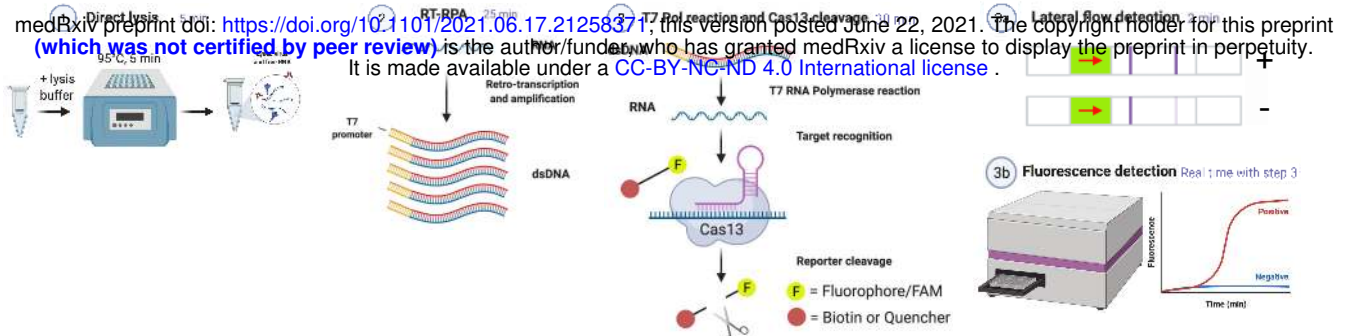
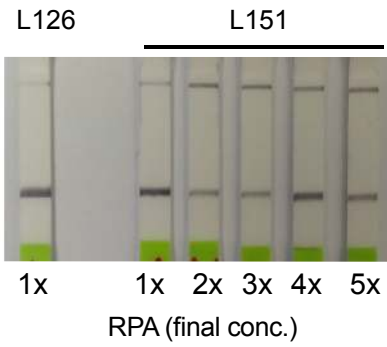


Figure S4

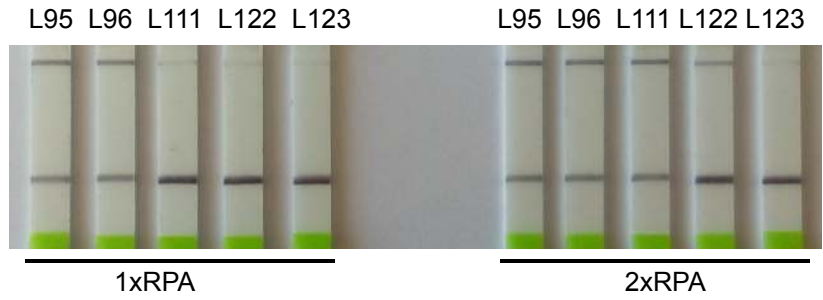
A



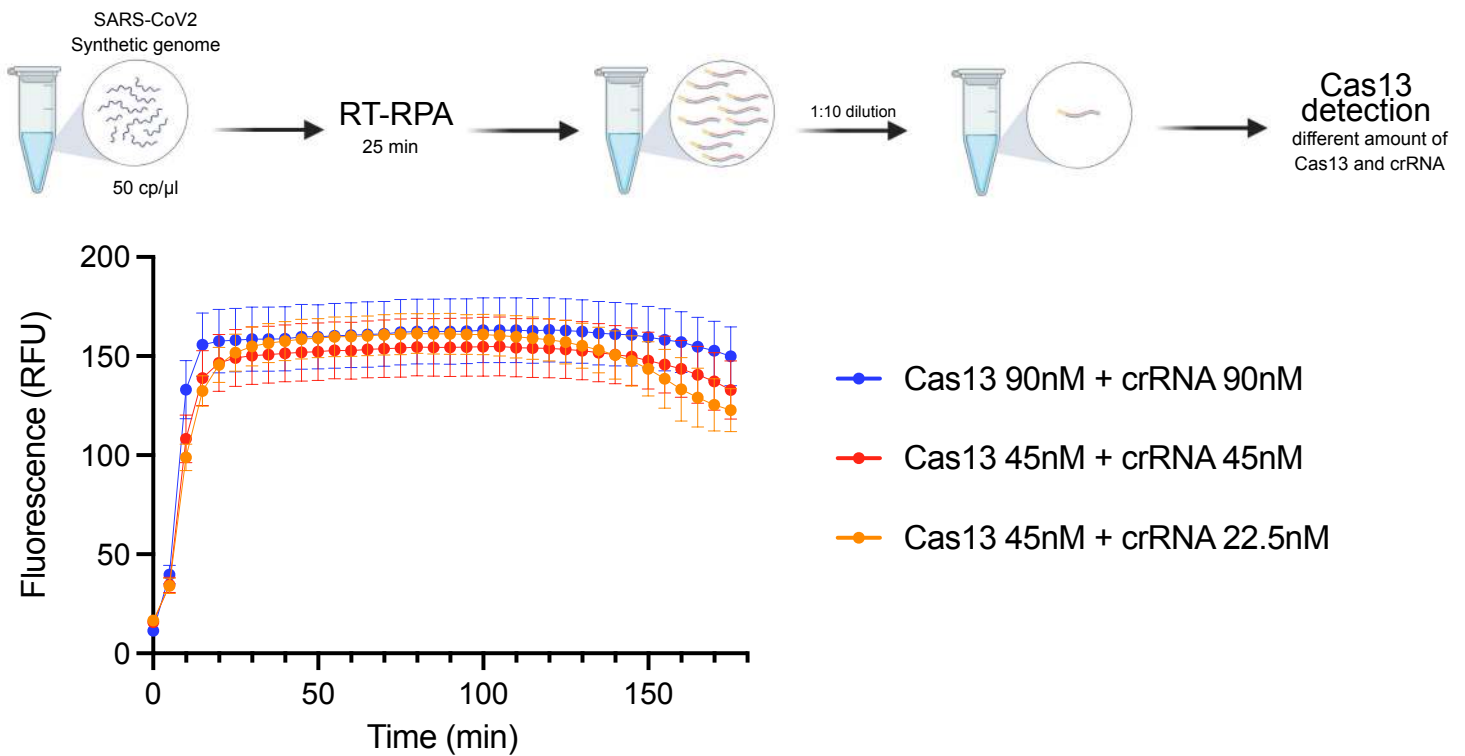
B



C



D



E

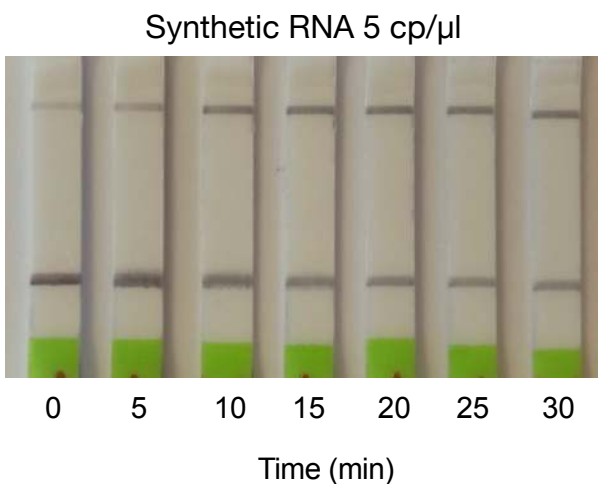
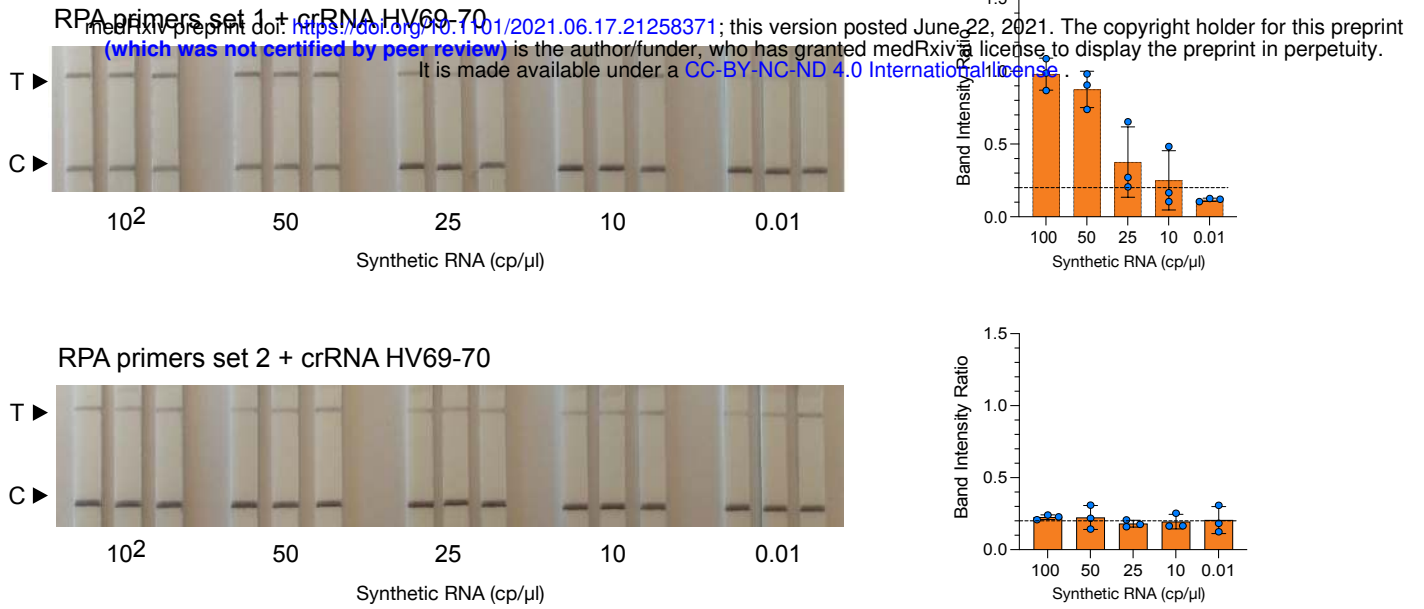
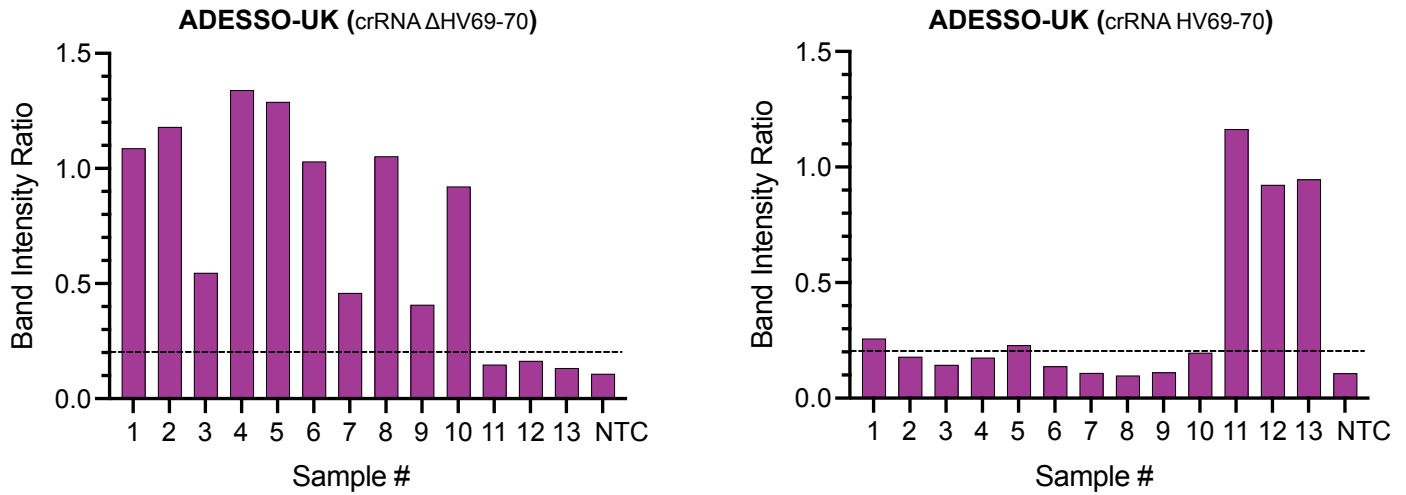


Figure S5

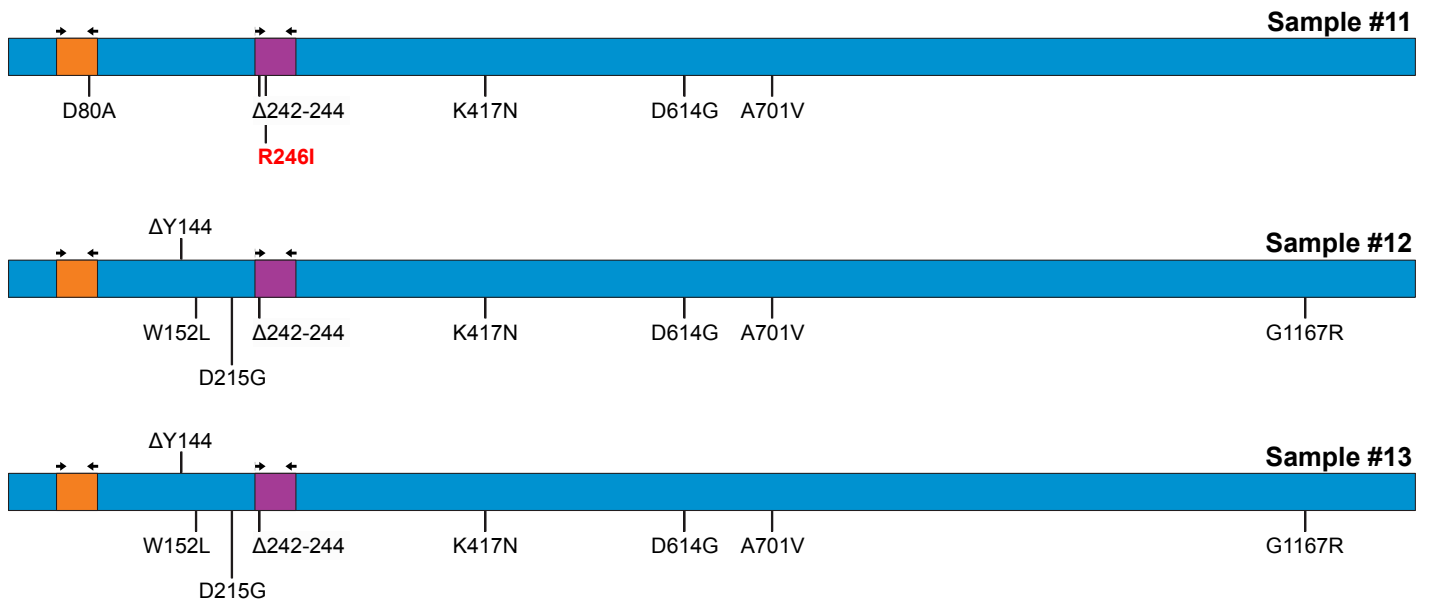
A



B



C



region recognised by ADESSO
region recognised by ADESSO-UK

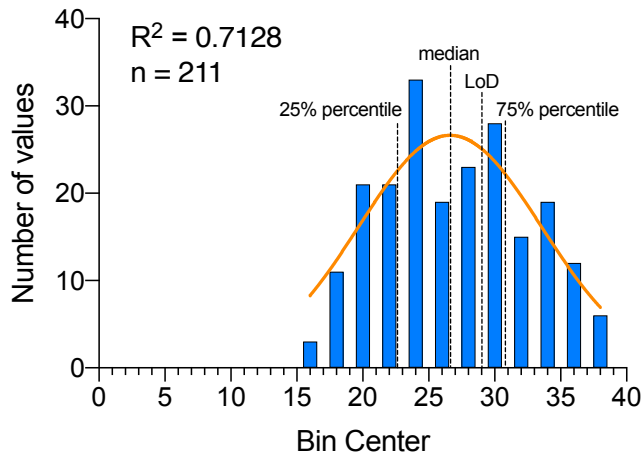
B.1.351
(South Africa variant)

Figure S6

A

medRxiv preprint doi: <https://doi.org/10.1101/2021.06.17.21258371>; this version posted June 22, 2021. The copyright holder for this preprint (which was not certified by peer review) is the author/funder, who has granted medRxiv a license to display the preprint in perpetuity. It is made available under a [CC-BY-NC-ND 4.0 International license](https://creativecommons.org/licenses/by-nc-nd/4.0/).

Frequency distribution Ct values



B

Cumulative Frequency distribution Ct values

